JOURNAL OF OPTIMIZATION THEORY AND APPLICATIONS: Vol. 50, No. 1, JULY 1986

Guidance Strategies for Near-Optimum Take-Off Performance in a Windshear[1,2,3]

A. MIELE,[4] T. WANG,[5] AND W. W. MELVIN[6]

Abstract. This paper is concerned with guidance strategies for near-optimum performance in a windshear. This is a wind characterized by sharp change in intensity and direction over a relatively small region of space. The take-off problem is considered with reference to flight in a vertical plane.

First, trajectories for optimum performance in a windshear are determined for different windshear models and different windshear intensities. Use is made of the methods of optimal control theory in conjunction with the dual sequential gradient-restoration algorithm (DSGRA) for optimal control problems. In this approach, global information on the wind flow field is needed.

Then, guidance strategies for near-optimum performance in a windshear are developed, starting from the optimal trajectories. Specifically, three guidance schemes are presented: (A) gamma guidance, based on the relative path inclination; (B) theta guidance, based on the pitch attitude angle; and (C) acceleration guidance, based on the relative acceleration. In this approach, local information on the wind flow field is needed.

---

[1] Portions of this were presented at the AIAA 24th Aerospace Sciences Meeting, Reno, Nevada, January 6–9, 1986. The authors are indebted to Boeing Commercial Aircraft Company, Seattle, Washington and to Pratt and Whittney Aircraft, East Hartford, Connecticut for supplying some of the technical data pertaining to this study.

[2] The authors are indebted to Dr. R. L. Bowles, NASA-Langley Research Center, Hampton, Virginia for helpful discussions. They are also indebted to Mr. Z. G. Zhao, Aero-Astronautics Group, Rice University, Houston, Texas for analytical and computational assistance.

[3] This research was supported by NASA-Langley Research Center, Grant No. NAG-1-516. This paper, a continuation of Ref.1, is based in part on Refs. 2–3.

[4] Professor of Astronautics and Mathematical Sciences, Aero-Astronautics Group, Rice University, Houston, Texas.

[5] Senior Research Associate, Aero-Astronautics Group, Rice University, Houston, Texas.

[6] Captain, Delta Airlines, Atlanta, Georgia; and Chairman, Airworthiness and Performance Committee, Air Line Pilots Association (ALPA), Washington, DC.

0022-3239/86/0700-0001$05.00/0

Next, several alternative schemes are investigated for the sake of completeness, more specifically: (D) constant alpha guidance; (E) constant velocity guidance; (F) constant theta guidance; (G) constant relative path inclination guidance; (H) constant absolute path inclination guidance; and (I) linear altitude distribution guidance.

Numerical experiments show that guidance schemes (A)-(C) produce trajectories which are quite close to the optimum trajectories. In addition, the near-optimum trajectories associated with guidance schemes (A)-(C) are considerably superior to the trajectories arising from the alternative guidance schemes (D)-(I).

An important characteristic of guidance schemes (A)-(C) is their simplicity. Indeed, these guidance schemes are implementable using available instrumentation and/or modification of available instrumentation.

Key Words. Guidance strategies, gamma guidance, theta guidance, acceleration guidance, flight mechanics, take-off, optimal trajectories, optimal control, feedback control, windshear problems, sequential gradient-restoration algorithm, dual sequential gradient-restoration algorithm.

1. Introduction

Low altitude windshear constitutes a considerable hazard in the take-off and landing of both civilian and military airplanes. For this reason, considerable research has been done on this problem over the past 15 years. Most of the research has been concerned with meteorology, instrumentation, aerodynamics, flight mechanics, and stability and control. Recently, optimal flight trajectories in the the presence of a windshear have been studied (Ref. 1). This opens the road to the development of guidance schemes for achieving near-optimum performance in a windshear (Refs. 2-3).

Previous Research. Previous research on the topics covered in this paper can be found in Refs. 4-40. For a general review of windshear studies, see Ref. 4. For the equations of motion without windshear, see Ref. 5; for the equations of motion with windshear, see Refs. 6-9. For windshear models, see Refs. 10-14.

Concerning trajectory optimization, for a recent overview of theoretical calculus of variations and optimal control, see Ref. 15. For algorithmic optimal control by means of gradient methods, see Refs. 16-20 (primal formulation) and Refs. 21-22 (dual formulation). For minimax optimal control, see Refs. 23-35; in particular, for aerospace applications of minimax optimal control see Refs. 24 and 31-35. Finally, for guidance schemes, see Refs. 14 and 36-40.

Present Research. This paper deals with guidance schemes for near-optimum performance in a windshear. The take-off problem is analyzed. In take-off, once an aircraft becomes airborne, the pilot has no choice but to fly through a windshear. His only control is the angle of attack. Indeed, it is logical to assume that, if a plane takes off under less-than-ideal weather conditions, the power setting is being held at that value which yields the maximum thrust.

First, trajectories for optimum performance in a windshear are determined for different windshear models and different windshear intensities. Use is made of the methods of optimal control theory in conjunction with the dual sequential gradient-restoration algorithm (DSGRA) for optimal control problems. In this approach, global information on the wind flow field is needed.

Then, guidance schemes for near-optimum performance in a windshear are developed, starting from the optimal trajectories. Specifically, three guidance schemes are presented: (A) gamma guidance, based on the relative path inclination; (B) theta guidance, based on the pitch attitude angle; and (C) acceleration guidance, based on the relative acceleration. In this approach, local information on the wind flow field is needed.

Schemes (A), (B), (C) are evaluated through numerical experiments (i) in order to determine whether the resulting trajectories are sufficiently close to the optimum trajectories and (ii) in order to compare the resulting trajectories with alternative guidance schemes. An important characteristic of Schemes (A), (B), (C) is their simplicity. Indeed, these guidance schemes are implementable using available instrumentation and/or modification of available instrumentation.

Outline. Section 2 contains the notations, and Section 3 contains the formulation of the problem. Section 4 pertains to optimum flight trajectories. Section 5 refers to guidance schemes for near-optimum flight trajectories, and Section 6 refers to alternative guidance schemes. A comparison between the various guidance schemes is presented in Section 7, and the conclusions are given in Section 8. Finally, the data for the examples are presented in the Appendix (Section 9).

2. Notations

Throughout the paper, the following notations are employed:

ARL = aircraft reference line;

D = drag force, lb;

g = acceleration of gravity, ft sec^{-2};

h = altitude, ft;

K = gain coefficient;
L = lift force, lb;
m = mass, lb ft^{-1} sec^2;
T = thrust force, lb;
V = relative velocity, ft sec^{-1};
V_e = absolute velocity, ft sec^{-1};
W = mg = weight, lb;
W = wind velocity, ft sec^{-1};
W_h = h-component of wind velocity, ft sec^{-1};
W_x = x-component of wind velocity, ft sec^{-1};
x = horizontal distance, ft.

Greek Symbols

α = relative angle of attack, rad;
α_e = absolute angle of attack, rad;
β = engine power setting;
γ = relative path inclination, rad;
γ_e = absolute path inclination, rad;
δ = thrust inclination, rad;
δ_e = elevator deflection, rad;
θ = pitch attitude angle, rad.

Subscripts

e = denotes Earth-fixed system;
l = denotes direction orthogonal to relative velocity;
le = denotes direction orthogonal to absolute velocity;
h = denotes h-direction;
x = denotes x-direction;
v = denotes direction of relative velocity;
ve = denotes direction of absolute velocity.

Superscripts

$\cdot$ = denotes derivative with respect to time;
$\rightarrow$ = denotes vector quantity;
$\sim$ = denotes nominal value.

3. Problem Formulation

This section pertains to the formulation of the problem. Specifically, the coordinate systems are presented in Section 3.1 and the equations of motion are given in Section 3.2. The approximations employed for the force terms are discussed in Section 3.3, and the approximations employed for the windshear terms are shown in Section 3.4. The inequality constraints on the angle of attack and its time derivative are presented in Section 3.5, and the boundary conditions are given in Section 3.6.

3.1. Coordinate Systems. In Ref. 1, three coordinate systems were considered: (i) the Earth-fixed system, (ii) the relative wind-axes system, and (iii) the absolute wind-axes system. It was assumed that flight takes place in a vertical plane.

Let $\vec{V}$ denote the velocity of the aircraft with respect to the airstream; let $\vec{W}$ denote the velocity of the airstream with respect to the Earth; and let $\vec{V}_e$ denote the velocity of the aircraft with respect to the Earth. With this understanding, the coordinate systems (i), (ii), (iii) are defined below (see Fig. 1).

In the Earth-fixed system Oxh, the point O is fixed with respect to the Earth; the x-axis is horizontal, positive in the sense of the motion; and the h-axis is orthogonal to the x-axis, hence vertical, positive upward.

In the relative wind-axes system Px_vy_l, the point P moves together with the aircraft; the x_v-axis has the direction of the relative velocity vector $\vec{V}$; and the y_l-axis has the direction of the lift vector $\vec{L}$.

In the absolute wind-axes system $Px_{ve}y_{le}$, the point P moves together with the aircraft; the x_{ve}-axis has the direction of the absolute velocity vector

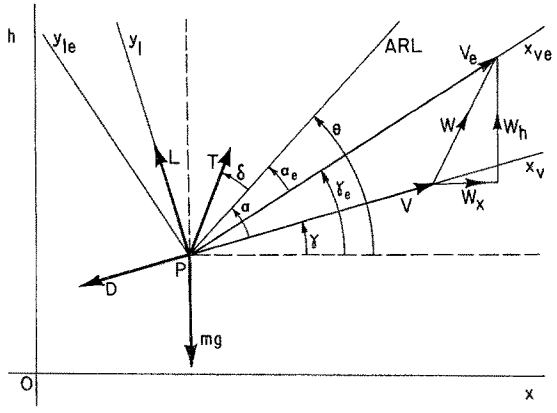

Fig. 1. Coordinate systems and force diagram.

$\vec{V}_e$; and the y_{le}-axis has the direction of the projected lift vector $\vec{L}_e$; the latter vector is obtained by projecting $\vec{L}$ in the direction orthogonal to x_{ve}.

3.2. Equations of Motion. Consistently with Ref. 1, we employ the following assumptions: (a) the aircraft is a particle of constant mass; (b) flight takes place in a vertical plane; (c) Newton's law is valid in an Earth-fixed system; and (d) the wind flow field is steady. Also consistently with Ref. 1, we make use of the relative wind-axes system. This is due to the fact that, in this system, the windshear terms appear explicitly in the equations of motion.

With the above premises, the equations of motion are written as follows:

$$\dot{x} = V\cos\gamma + W_x, \tag{1a}$$

$$\dot{h} = V\sin\gamma + W_h, \tag{1b}$$

$$\begin{aligned}\dot{V} = {} & (T/m)\cos(\alpha+\delta) - D/m - g\sin\gamma \\ & -[(\partial W_x/\partial x)(V\cos\gamma + W_x) + (\partial W_x/\partial h)(V\sin\gamma + W_h)]\cos\gamma \\ & -[(\partial W_h/\partial x)(V\cos\gamma + W_x) + (\partial W_h/\partial h)(V\sin\gamma + W_h)]\sin\gamma,\end{aligned} \tag{1c}$$

$$\begin{aligned}\dot{\gamma} = {} & (T/mV)\sin(\alpha+\delta) + L/mV - (g/V)\cos\gamma \\ & +[(\partial W_x/\partial x)(V\cos\gamma + W_x) + (\partial W_x/\partial h)(V\sin\gamma + W_h)](1/V)\sin\gamma \\ & -[(\partial W_h/\partial x)(V\cos\gamma + W_x) + (\partial W_h/\partial h)(V\sin\gamma + W_h)](1/V)\cos\gamma.\end{aligned} \tag{1d}$$

These equations must be supplemented by the functional relations

$$D = D(h, V, \alpha), \tag{2a}$$

$$L = L(h, V, \alpha), \tag{2b}$$

$$T = T(h, V, \beta), \tag{2c}$$

$$W_x = W_x(x, h), \tag{2d}$$

$$W_h = W_h(x, h), \tag{2e}$$

and by the analytical relations

$$V_{ex} = V\cos\gamma + W_x, \tag{3a}$$

$$V_{eh} = V\sin\gamma + W_h, \tag{3b}$$

$$V_e = \sqrt{(V_{ex}^2 + V_{eh}^2)}, \tag{3c}$$

$$\gamma_e = \arctan(V_{eh}/V_{ex}), \tag{3d}$$

$$\theta = \alpha + \gamma, \tag{3e}$$

$$\alpha_e = \alpha + \gamma - \gamma_e. \tag{3f}$$

For a given value of the thrust inclination δ, the differential system (1)-(2) involves four state variables (the horizontal distance x, the altitude h, the velocity V, and the relative path inclination γ) and two control variables (the angle of attack α and the power setting β). However, the number of control variables reduces to one (the angle of attack α), if the power setting β is specified in advance.

The quantities defined by the analytical relations (3) can be computed a posteriori, once the values of x, h, V, γ, α, β are known. Indeed, V_{ex}, V_{eh}, V_e, γ_e are known functions of the state variables defined by Eqs. (3a)-(3d). Analogously, θ, α_e are known functions of the state variables and the control variables defined by Eqs. (3e)-(3f).

3.3. Approximations for the Force Terms. Here, we discuss the approximations employed in the description of the forces acting on the aircraft, namely, the thrust, the drag, the lift, and the weight. Because the trajectories under investigation involve relatively minor variations of the altitude, the air density is assumed to be constant.

Thrust. The thrust T is approximated with the quadratic function

$$T = A_0 + A_1 V + A_2 V^2, \tag{4}$$

where V is the relative velocity and where the coefficients A_0, A_1, A_2 depend on the altitude of the runway, the ambient temperature, and the engine power setting. For given runway altitude, ambient temperature, and engine power setting, the coefficients A_0, A_1, A_2 can be determined with a least-square fit of manufacturer-supplied data over a given interval of velocities.

Drag. The drag D is written in the form

$$D = (1/2) C_D \rho S V^2, \tag{5}$$

where ρ is the air density, S is a reference surface, V is the relative velocity, and C_D is the drag coefficient. In turn, the drag coefficient is approximated with the quadratic function

$$C_D = B_0 + B_1 \alpha + B_2 \alpha^2, \qquad \alpha \leq \alpha_*, \tag{6}$$

where α is the relative angle of attack and where the coefficients B_0, B_1, B_2 depend on the flap setting and the undercarriage position (gear up or gear down). For given flap setting and given undercarriage position, the coefficients B_0, B_1, B_2 can be determined with a least-square fit of manufacturer-supplied data over the interval $0 \leq \alpha \leq \alpha_*$.

Lift. The lift L is written in the form

$$L = (1/2) C_L \rho S V^2, \tag{7}$$

where ρ is the air density, S is a reference surface, V is the relative velocity, and C_L is the lift coefficient. In turn, the lift coefficient is approximated as follows:

$$C_L = C_0 + C_1 \alpha, \qquad \alpha \leq \alpha_{**}, \tag{8a}$$

$$C_L = C_0 + C_1 \alpha + C_2 (\alpha - \alpha_{**})^2, \qquad \alpha_{**} \leq \alpha \leq \alpha_*, \tag{8b}$$

where α is the relative angle of attack and where the coefficients C_0, C_1, C_2 depend on the flap setting and the undercarriage position (gear up or gear down). For given flap setting and given undercarriage position, the coefficients C_0, C_1 can be determined with a least-square fit of manufacturer-supplied data over the interval $0 \leq \alpha \leq \alpha_{**}$. With C_0, C_1 known, the coefficient C_2 is determined with a least-square fit of manufacturer-supplied data over the interval $\alpha_{**} \leq \alpha \leq \alpha_*$.

Weight. The mass m is regarded to be constant. Hence, the weight $W = mg$ is regarded to be constant.

3.4. Approximations for the Windshear. Here, we discuss some of the approximations employed in the description of the windshear,. We observe that, under the assumption that the wind flow field is steady, the wind components W_x, W_h have the form

$$W_x = W_x(x, h), \qquad W_h = W_h(x, h). \tag{9}$$

Windshear Models. Over the past several years, considerable attention has been given to the study of a severe meteorological condition known as a microburst (Refs. 4 and 6-14). This condition involves a descending column of air, which then spreads horizontally in the neighborhood of the ground. This condition is hazardous, because an aircraft in take-off or landing might encounter a headwind coupled with a downdraft, followed by a tailwind coupled with a downdraft. A qualitative example of the vertical cross section of a microburst is shown in Fig. 2.

It is clear that, in order to perform realistic analyses of take-off and landing under severe meteorological conditions, one must represent wind flow fields of the type shown in Fig. 2. The representation of the wind flow field can be obtained from the combination of theory and experimental measurements.

From an engineering point of view, a simplifying observation can be made. In the neighborhood of the ground, the vertical component of the

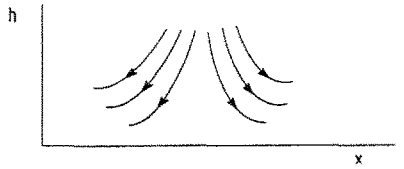

Fig. 2. Typical cross section of the wind flow field (microburst).

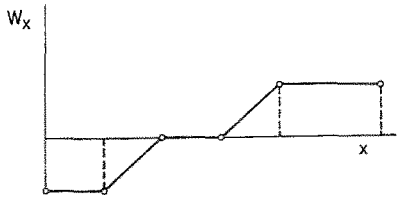

Fig. 3. Idealized distribution of the horizontal component of the wind velocity (W_x positive for tailwind, negative for headwind).

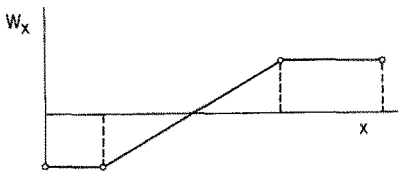

Fig. 4. Idealized distribution of the horizontal component of the wind velocity (W_x positive for tailwind, negative for headwind).

wind velocity is small by comparison with the horizontal component (Ref. 14). Therefore, the idea arises of studying take-off and landing in the presence of windshear by considering only the horizontal component of the wind velocity. This simplified wind model is represented by

$$W_x = W_x(x), \qquad W_h = 0 \tag{10}$$

and is shown in Figs. 3–4. Figure 3 is an idealization of the near-the-ground behavior of the microburst model shown in Fig. 2. In turn, Fig. 4 is a particular case of Fig. 3.

Figure 4 represents the transition from a uniform headwind to a uniform tailwind. It is governed by the following equations

$$W_x = -k, \qquad x \le a, \tag{11a}$$

$$W_x = -k + 2k(x-a)/(b-a), \qquad a \le x \le b, \tag{11b}$$

$$W_x = k, \qquad x \ge b. \tag{11c}$$

Therefore, the wind velocity difference is

$$\Delta W_x = 2k \tag{12a}$$

and the windshear intensity is

$$\Delta W_x/\Delta x = 2k/(b-a). \tag{12b}$$

Equations (11)-(12) represent a three-parameter family of wind models, the parameters being a, b, k. Note that a is associated with the windshear onset, and b is associated with the windshear termination. If a and b are given, Eqs. (11)-(12) represent a one-parameter family of wind models. The parameter k determines both the wind velocity difference (12a) and the windshear intensity (12b).

Table 1 shows the values of ΔW_x and $\Delta W_x/\Delta x$ for several values of the parameter k, under the assumption that $b-a=4{,}000$ ft. Small values of k correspond to windshears that are survivable, while large values of k correspond to windshears that are not survivable.

The last column of Table 1, labeled "Remarks", attempts to correlate the windshear intensity $\Delta W_x/\Delta x$ with several recent windshear episodes. The correlation is qualitative and is merely done to establish a reference frame for the numerical examples of Sections 4–6.

Smoothing Technique. Inspection of Eqs. (1) shows that the first derivatives of the wind components are present in the dynamical equations. Therefore, if gradient-type algorithms are used to optimize flight trajectories in the presence of windshear (Refs. 16–22), one needs the second derivatives of the wind components. For the idealized wind models considered in Figs. 3–4, the first derivatives are discontinuous at the corner points; therefore,

Table 1. Wind velocity difference and windshear intensity, $b-a=4{,}000$ ft.

k (ft sec^{-1})	ΔW_x (ft sec^{-1})	$\Delta W_x/\Delta x$ (sec^{-1})	Remarks
10	20	0.005	
20	40	0.010	JAWS
30	60	0.015	
40	80	0.020	CAL 063
50	100	0.025	DAL 191
60	120	0.030	EAL 066, PAA 759
70	140	0.035	
80	160	0.040	CAL 426
90	180	0.045	
100	200	0.050	Andrews AFB

the second derivatives do not exist at these points. In the real world, this situation is not acceptable. This being the case, a smoothing technique is needed to ensure the continuity of both the first derivatives and the second derivatives of the wind components. This smoothing technique was discussed in Ref. 1 and is not repeated here, for the sake of brevity.

3.5. Inequality Constraints. The angle of attack α appearing in Eqs. (1)-(3), (6), (8) is subject to the inequality

$$\alpha \leq \alpha_*, \tag{13}$$

where α_* is prescribed upper bound. In addition, the time derivative of the angle of attack is subject to the inequality

$$-C \leq \dot{\alpha} \leq +C, \tag{14}$$

where C is a prescribed, positive constant.

For the optimal trajectories of Section 4, Ineqs. (13)-(14) are satisfied indirectly via transformation techniques, discussed in Ref. 1. In particular, Ineq. (14) requires the conversion of α from a control variable into a state variable.

For the guidance schemes of Sections 5-6, Ineq. (13) is satisfied directly. On the other hand, Ineq. (14) is satisfied indirectly through the proper choice of the gain coefficient K.

3.6. Boundary Conditions. First, we refer to the optimal trajectories of Section 4. Concerning the initial conditions, it is assumed that the values of x, h, V, γ, α are specified at $t=0$; that is,

$$x(0)=x_0, \qquad h(0)=h_0, \qquad V(0)=V_0, \qquad \gamma(0)=\gamma_0, \tag{15}$$

$$\alpha(0)=\alpha_0. \tag{16}$$

We note that the specification of the initial value of α is possible in the light of the transformation technique ensuing from Ineq. (14); see Ref. 1.

Concerning the final conditions, it is assumed that the value of γ is specified at $t=\tau$, that is,

$$\gamma(\tau)=\gamma_0. \tag{17}$$

The remaining state variables are free at the final point. The final time τ is chosen to be large enough to correspond to a no-windshear condition.

Clearly, use of (17) means that, at the final point, one intends to restore the initial value of the path inclination. In accordance with the terminology employed in Ref. 1, this type of boundary condition is called boundary condition BC1.

Next, we refer to the guidance schemes of Sections 5-6. At the initial time $t=0$, it is assumed that the values of x, h, V, γ are specified; that is, Eqs. (15) hold, while Eq. (16) is disregarded. At the final time $t=\tau$, it is assumed that the values of x, h, V, γ are free; in particular, Eq. (17) is disregarded; nevertheless, approximate enforcement of (17) can take place through the proper choice of the guidance law and the gain coefficient K.

4. Optimum Flight Trajectories

This section pertains to optimum flight trajectories, Specifically, the optimal control problem is formulated in Section 4.1, and the sequential gradient-restoration algorithm is briefly mentioned in Section 4.2. The numerical results for the optimal flight trajectories are given in Section 4.3, with particular reference to the effect of the windshear model and the effect of the windshear intensity.

4.1. Optimal Control Problem. We refer to the system described in Section 3. We assume that the wind flow field is known in advance. We assume that the power setting is given, so that the only control is the angle of attack, treated here as a state variable. In addition, we assume that the initial conditions (15)-(16) are given in conjunction with the final condition (17). With this understanding and with particular reference to take-off trajectories, we formulate the following optimization problem (Ref. 1).

Problem (P7). Minimize the peak value of the modulus of the difference between the relative path inclination and a reference value, assumed constant. In this problem, the performance index is given by

$$I=\max_t|\gamma-\gamma_R|, \qquad 0\leq t\leq\tau, \tag{18a}$$

where

$$\gamma_R=\gamma_0. \tag{18b}$$

This is a minimax problem or Chebyshev problem of optimal control. It can be reformulated as a Bolza problem of optimal control (Ref. 35), in which one minimizes the integral performance index

$$J=\int_0^\tau(\gamma-\gamma_R)^q\,dt, \tag{18c}$$

for large values of the positive, even exponent q.

Remark. In Ref. 1, eight fundamental optimization problems were formulated [Problems (P1)-(P8)]. They were solved for four types of boundary conditions (boundary conditions BC0, BC1, BC2, BC3). Among the trajectories investigated, the trajectory solving Problem (P7) for boundary condition BC1 proved to be of particular interest. This is why the present paper refers to this particular optimal trajectory. The basic idea is to develop guidance schemes which allow the aircraft to approach the behavior of the optimal trajectory solving Problem (P7) for boundary condition BC1.

4.2. Sequential Gradient-Restoration Algorithm. Problem (P7) can be solved using the family of sequential gradient-restoration algorithms for optimal control problems (SGRA, Refs. 16-22), in either the primal formulation (PSGRA, Refs. 16-20) or the dual formulation (DSGRA, Refs. 21-22). Regardless of whether the primal formulation is used or the dual formulation is used, sequential gradient-restoration algorithms involve a sequence of two-phase cycles, each cycle including a gradient phase and a restoration phase. In the gradient phase, the value of the augmented functional is decreased, while avoiding excessive constraint violation. In the restoration phase, the value of the constraint error is decreased, while avoiding excessive change in the value of the functional. In a complete gradient-restoration cycle, the value of the functional is decreased, while the constraints are satisfied to a preselected degree of accuracy. Thus, a succession of suboptimal solutions is generated, each new solution being an improvement over the previous one from the point of view of the value of the functional being minimized.

The convergence conditions are represented by the relations

$$P \leq \epsilon_1, \qquad Q \leq \epsilon_2. \tag{19}$$

Here, P is the norm squared of the error in the constraints, Q is the norm squared of the error in the optimality conditions, and ϵ_1, ϵ_2 are preselected, small, positive numbers.

In this work, the sequential gradient-restoration algorithm is employed in conjunction with the dual formulation. The algorithmic details can be found in Refs. 21-22. They are omitted here, for the sake of brevity.

4.3. Numerical Results. Optimal flight trajectories were computed for a Boeing B-727 aircraft powered by three JT8D-17 turbofan engines. It was assumed that: (i) the aircraft has become airborne from a runway located at sea-level altitude; (ii) the ambient temperature is 100 deg Fahrenheit; (iii) the gear is up; (iv) the flap setting is $\delta_F = 15$ deg; and (v) the engines are operating at maximum power setting. The complete data for the examples can be found in Section 9. In particular, the final time is $\tau = 40$ sec. This is about twice the duration of the windshear encounter (18 sec).

Problem (P7) was solved employing the sequential gradient-restoration algorithm in connection with the dual formulation (DSGRA, Refs. 21–22). This algorithm was programmed in FORTRAN IV, and the numerical results were obtained in double-precision arithmetic. Computations were performed at Rice University using an NAS-AS-9000 computer.

The interval of integration was divided into 100 steps. The differential systems were integrated using Hamming's modified predictor-corrector method, with a special Runge-Kutta starting procedure. Definite integrals were computed using a modified Simpson's rule. Linear algebraic systems were solved using a standard Gaussian elimination routine.

Several combinations of windshear models and windshear intensities were considered (see Refs. 2–3). For computational efficiency, the state variables and the time were suitably scaled. For Problem (P7), the functional being minimized was suitably scaled. The following stopping conditions were employed for the dual sequential gradient-restoration algorithm:

$$P \leq E-10, \qquad Q \leq E-08, \tag{20}$$

where P denotes the constraint error and Q denotes the error in the optimality conditions.

The results are given in Figs. 5–6. Each figure contains six parts: the wind velocity W_x; the flight altitude h; the relative velocity V; the relative path inclination γ; the angle of attack α; and the pitch attitude angle θ.

Effect of the Windshear Model. We refer to the optimal trajectories of Problem (P7), minimax $|\Delta\gamma|$, in connection with boundary condition model BC1, wind velocity difference $\Delta W_x = 80$ ft sec^{-1}, windshear intensity $\Delta W_x/\Delta x = 0.020$ sec^{-1}. We consider the windshear models WS1, WS2, WS3 (see Fig. 5). We recall that, in model WS1, the windshear starts at $x = 0$ ft; in model WS2, the windshear starts at $x = 700$ ft; in model WS3, the windshear starts at $x = 1{,}700$ ft (see Section 9 for details).

From Fig. 5, we see that a similarity of behavior exists between the optimal trajectories associated with windshear models WS1, WS2, WS3. In particular, the following points must be noted: (i) the altitude distribution exhibits a monotonic behavior, regardless of the windshear model; (ii) for the windshear portion of the flight, the angle of attack distribution is qualitatively the same for models WS1, WS2, WS3; specifically, the $\alpha(t)$ distribution for models WS2, WS3 can be obtained from the $\alpha(t)$ distribution for model WS1 by means of a timewise parallel displacement; an analogous remark holds for the velocity distribution; it is possible that the combined behavior of the angle of attack distribution and the velocity distribution might be of interest for the development of a guidance scheme; (iii) for the

prewindshear portion of the flight, it is desirable to slightly decrease the angle of attack, while simultaneously increasing the relative velocity.

Effect of the Windshear Intensity. We refer to the optimal trajectories of Problem (P7), minimax $|\Delta\gamma|$, in connection with boundary condition model BC1, windshear model WS1. We consider the wind velocity differences $\Delta W_x = 80, 100, 120, 140$ ft sec^{-1}, corresponding to the windshear intensities $\Delta W_x/\Delta x = 0.020, 0.025, 0.030, 0.035$ sec^{-1} (see Fig. 6).

From Fig. 6, the following points must be noted: (i) as the wind velocity difference increases, the altitude distribution exhibits a considerable change, while this is not the case with the velocity distribution and the angle of attack distribution; (ii) if the wind velocity difference is $\Delta W_x = 80$ ft sec^{-1} or $\Delta W_x = 100$ ft sec^{-1}, the altitude distribution has a monotonically climbing behavior; if the wind velocity difference is increased to $\Delta W_x = 120$ ft sec^{-1}, the altitude distribution is characterized by a dip, so that the optimal trajectory is dangerously close to the ground; if the wind velocity difference is further increased to $\Delta W_x = 140$ ft sec^{-1}, the optimal trajectory hits the ground; (iii) with reference to the cases where $\Delta W_x = 120$ ft sec^{-1} and $\Delta W_x = 140$ ft sec^{-1}, the windshear inertia force is larger than both the drag and the thrust over a considerable time interval; this explains why the optimal trajectory for $\Delta W_x = 120$ ft sec^{-1} is dangerously close to the ground, while the optimal trajectory for $\Delta W_x = 140$ ft sec^{-1} hits the ground; (iv) for the windshear portion of the flight, the angle of attack distribution is relatively insensitive to the wind velocity difference ΔW_x; an analogous remark holds for the velocity distribution; it is possible that the combined behavior of the angle of attack distribution and the velocity distribution might be of interest for the development of a guidance scheme.

Comment. From the previous numerical results, certain concepts seem to emerge, relative to the windshear portion of the flight trajectory: (i) low angles of attack correspond to high velocities and high angles of attack correspond to low velocities; and (ii) the angle of attack boundary is reached at the minimum velocity point, that is, about the time when the windshear ends. Concepts (i) and (ii) appear to be true, regardless of the windshear model and the windshear intensity.

5. Near-Optimum Guidance Schemes

This section pertains to guidance schemes for near-optimum flight trajectories. Specifically, (A) the gamma guidance is presented in Section 5.1; (B) the theta guidance is presented in Section 5.2; and (C) the acceleration guidance is presented in Section 5.3. The implementation of the

guidance laws is discussed in Section 5.4. Then, the numerical results for the near-optimum guidance schemes are given in Section 5.5, with particular reference to the effect of the windshear model and the effect of the windshear intensity.

5.1. Gamma Guidance. Scheme (A). Here, we present a guidance scheme, based on path inclination, whose objective is to approximate the behavior of the optimal trajectories in a windshear. The guidance scheme relies on certain basic facts, which can be established by inspection of the optimal trajectories presented in Fig. 5-6:

(i) it appears that there is some relation between the angle of attack and the velocity; it also appears that this relation is relatively insensitive to the windshear model and the windshear intensity; more specifically, low angles of attack correspond to high velocities, and high angles of attack correspond to low velocities;

(ii) it appears that the average path inclination which can be maintained in a windshear depends strongly on the windshear intensity; more specifically, if the windshear intensity is zero, the average path inclination is equal to the initial value γ_0; if the windshear intensity increases, the average path inclination decreases, tending to zero when $\Delta W_x/\Delta x = 0.030\ \text{sec}^{-1}$, $\Delta W_x = 120\ \text{ft sec}^{-1}$.

From facts (i) and (ii), one surmises that the nominal values of the angle of attack and the path inclination can be described by relations of the form

$$\tilde{\alpha} = \tilde{\alpha}(V), \tag{21a}$$

$$\tilde{\gamma} = \tilde{\gamma}(\dot{W}_x), \tag{21b}$$

where

$$\dot{W}_x = (\partial W_x/\partial x)(V\cos\gamma + W_x). \tag{21c}$$

These relations indicate that the gamma guidance law should have the form

$$\gamma = \tilde{\gamma}(\dot{W}_x). \tag{22}$$

In turn, (22) can be implemented through the feedback control law

$$\alpha - \tilde{\alpha}(V) = -K[\gamma - \tilde{\gamma}(\dot{W}_x)], \qquad \alpha \leq \alpha_*, \tag{23}$$

where K is the gain coefficient.

Nominal Angle of Attack. Let the dynamical equations (1c) and (1d) be rewritten in the alternative form

$$\dot{V} = (T/m)\cos(\alpha+\delta) - D/m - g\sin\gamma - \dot{W}_x\cos\gamma, \tag{24a}$$

$$\dot{\gamma} = (T/mV)\sin(\alpha+\delta) + L/mV - (g/V)\cos\gamma + (\dot{W}_x/V)\sin\gamma. \tag{24b}$$

This form arises upon considering (21c) and the assumption that W_h is negligible.

Next, focus attention on (24b) and assume that, along a large portion of the optimal trajectory, the path inclination is sufficiently small, so that

$$\cos\gamma \cong 1, \tag{25a}$$

$$\dot{W}_x \sin\gamma \cong \dot{W}_x \gamma \ll g, \tag{25b}$$

$$\dot{\gamma} \ll g/V. \tag{25c}$$

Under these assumptions, (24b) yields the following nondifferential equation:

$$T\sin(\alpha+\delta)+L-mg=0, \tag{26}$$

which supplies implicitly the function (21a).

Next, we employ the representation (4) for the thrust and the representation (7)-(8) for the lift, namely,

$$T=A_0+A_1V+A_2V^2, \tag{27a}$$

$$L=(1/2)(C_0+C_1\alpha)\rho SV^2, \qquad \alpha\le\alpha_{**}, \tag{27b}$$

$$L=(1/2)[C_0+C_1\alpha+C_2(\alpha-\alpha_{**})^2]\rho SV^2, \qquad \alpha_{**}\le\alpha\le\alpha_*. \tag{27c}$$

Also, we expand the trigonometric term $\sin(\alpha+\delta)$ in Taylor series as follows:

$$\sin(\alpha+\delta)\cong(\alpha+\delta). \tag{28}$$

From (26)-(28), we obtain the following algebraic equations:

$$D_0+D_1\alpha=0, \qquad \alpha\le\alpha_{**}, \tag{29a}$$

$$E_0+E_1(\alpha-\alpha_{**})+E_2(\alpha-\alpha_{**})^2=0, \qquad \alpha_{**}\le\alpha\le\alpha_*, \tag{29b}$$

which admit the solutions

$$\alpha=-D_0/D_1, \qquad \alpha\le\alpha_{**}, \tag{30a}$$

$$\alpha=\alpha_{**}+(1/2E_2)[-E_1+\sqrt{(E_1^2-4E_0E_2)}], \qquad \alpha_{**}\le\alpha\le\alpha_*. \tag{30b}$$

The coefficients D_0, D_1 and E_0, E_1, E_2 depend on the state variables. They are given by

$$D_0=-1+(\delta/mg)(A_0+A_1V+A_2V^2)+(C_0\rho S/2mg)V^2, \tag{31a}$$

$$D_1=(1/mg)(A_0+A_1V+A_2V^2)+(C_1\rho S/2mg)V^2, \tag{31b}$$

and

$$E_0 = D_0 + D_1 \alpha_{**}, \tag{32a}$$

$$E_1 = D_1, \tag{32b}$$

$$E_2 = (C_2 \rho S / 2mg) V^2. \tag{32c}$$

Equations (30)-(32) supply explicitly the function (21a). For the Boeing B-727 aircraft and for the data of Section 9, the nominal angle of attack $\tilde{\alpha} = \tilde{\alpha}(V)$ is shown in Table 2.

Nominal Path Inclination. The nominal path inclination is described by the following relations:

$$\tilde{\gamma} = \gamma_0, \qquad \dot{W}_x / g \leq 0, \tag{33a}$$

$$\tilde{\gamma} = \gamma_0 (1 - 4 \dot{W}_x / g), \qquad 0 \leq \dot{W}_x / g \leq 13/56, \tag{33b}$$

$$\tilde{\gamma} = \gamma_0 / 14, \qquad \dot{W}_x / g \geq 13/56, \tag{33c}$$

whose justification is given below. If the wind gradient is negative or zero (therefore, favorable), the path inclination should be be kept constant [see (33a)]. If the wind gradient is large positive (therefore, very unfavorable),

Table 2. Gamma guidance, nominal angle of attack.

V (ft sec^{-1})	$\tilde{\alpha}$ (deg)
200	16.00
210	16.00
220	16.00
230	16.00
232.63	16.00
240	14.51
250	13.06
259.57	12.00
260	11.96
270	11.03
280	10.19
290	9.43
300	8.74
310	8.11
320	7.54
330	7.02
340	6.54
350	6.10

the path inclination should be kept at a small positive value [about 0.5 deg, see (33c)]. If the wind gradient is moderate positive, Eq. (33b) establishes a linear dependence of $\tilde{\gamma}$ on the windshear intensity. Note that $\tilde{\gamma}$ given by (33b) vanishes for $\dot{W}_x/g = 1/4$, corresponding to $\Delta W_x/\Delta x = 0.030\,\text{sec}^{-1}$. However, the value $\tilde{\gamma} = 0$ is undesirable and is prevented by (33c). The values of the nominal path inclination $\tilde{\gamma} = \tilde{\gamma}(\dot{W}_x)$ are shown in Table 3.

5.2. Theta Guidance. Scheme (B). Here, we present a guidance scheme, based on pitch attitude angle, whose objective is to approximate the behavior of the optimal trajectories in a windshear. The theta guidance scheme is similar to the gamma guidance scheme, but perhaps easier to implement in actual flight.

Omitting the details, the nominal values of the angle of attack and the pitch attitude angle can be described by relations of the form

$$\tilde{\alpha} = \tilde{\alpha}(V), \tag{34a}$$

$$\tilde{\theta} = \tilde{\theta}(\dot{W}_x, V), \tag{34b}$$

where $\dot{W}_x$ is supplied by Eq. (21c). These relations indicate that the theta guidance law should have the form

$$\theta = \tilde{\theta}(\dot{W}_x, V), \tag{35}$$

with the implication that

$$\alpha = \tilde{\theta}(\dot{W}_x, V) - \gamma, \qquad \alpha \leq \alpha_*. \tag{36}$$

Table 3. Gamma guidance, nominal path inclination.

$\dot{W}_x/g$	$\tilde{\gamma}/\gamma_0$
−0.250	1.000
−0.200	1.000
−0.150	1.000
−0.100	1.000
−0.050	1.000
0.000	1.000
0.050	0.800
0.100	0.600
0.150	0.400
0.200	0.200
0.232	0.071
0.250	0.071
0.300	0.071

Alternatively, (35) can be implemented through the feedback control law

$$\alpha - \tilde{\alpha}(V) = -K[\theta - \tilde{\theta}(\dot{W}_x, V)], \qquad \alpha \leq \alpha_*, \tag{37}$$

where K is the gain coefficient. In Eqs. (36)-(37), the nominal pitch attitude angle $\tilde{\theta}(\dot{W}_x, V)$ is given by

$$\tilde{\theta}(\dot{W}_x, V) = \tilde{\gamma}(\dot{W}_x) + \tilde{\alpha}(V), \tag{38}$$

where the function $\tilde{\gamma}(\dot{W}_x)$ is supplied by Eqs. (33). The nominal angle of attack $\tilde{\alpha}(V)$ is the same as in the gamma guidance scheme. Therefore, it is supplied by Eqs. (30)-(32).

5.3. Acceleration Guidance. Scheme (C). Here, we present a guidance scheme, based on relative acceleration, whose objective is to approximate the behavior of the optimal trajectories in a windshear. The guidance scheme relies on the fact that, for the windshear portion of the flight, the relative acceleration is approximately proportional to the windshear intensity.

The acceleration guidance law has the form

$$\dot{V} + C\dot{W}_x \cos\gamma = 0, \tag{39}$$

which determines the angle of attack in terms of the state variables and the windshear intensity. Upon combining (24a) and (39), and upon eliminating $\dot{V}$, we obtain the following relation:

$$T\cos(\alpha + \delta) - D - mg\sin\gamma - m(1 - C)\dot{W}_x \cos\gamma = 0. \tag{40}$$

Next, we employ the representation (4) for the thrust and the representation (6) for the drag, namely,

$$T = A_0 + A_1 V + A_2 V^2, \tag{41a}$$

$$D = (1/2)(B_0 + B_1\alpha + B_2\alpha^2)\rho S V^2, \tag{41b}$$

and we expand the trigonometric term $\cos(\alpha + \delta)$ in Taylor series as follows:

$$\cos(\alpha + \delta) \cong 1 - (1/2)(\alpha + \delta)^2. \tag{42}$$

From (40)-(42), we obtain the following quadratic equation:

$$F_0 + F_1\alpha + F_2\alpha^2 = 0, \qquad \alpha \leq \alpha_*, \tag{43}$$

which admits the solution

$$\alpha = (1/2F_2)[-F_1 + \sqrt{(F_1^2 - 4F_0F_2)}], \qquad \alpha \leq \alpha_*. \tag{44}$$

The coefficients F_0, F_1, F_2 depend on the state variables and the intensity of the windshear. They are given by

$$F_0 = [(-2+\delta^2)/2mg](A_0 + A_1 V + A_2 V^2) + (B_0 \rho S/2mg) V^2 + \sin\gamma + (1-C)(\dot{W}_x/g)\cos\gamma, \tag{45a}$$

$$F_1 = (\delta/mg)(A_0 + A_1 V + A_2 V^2) + (B_1 \rho S/2mg) V^2, \tag{45b}$$

$$F_2 = (1/2mg)(A_0 + A_1 V + A_2 V^2) + (B_2 \rho S/2mg) V^2. \tag{45c}$$

Alternatively, (39) can be implemented through the feedback control law

$$\alpha - \tilde{\alpha}(V) = -K[-\dot{V} - C\dot{W}_x \cos\gamma], \qquad \alpha \leq \alpha_*, \tag{46}$$

where K is the gain coefficient. In Eq. (46), the nominal angle of attack $\tilde{\alpha}(V)$ is the same as in the gamma guidance scheme. Therefore, it is supplied by Eqs. (30)-(32). The computation of $\dot{W}_x$ is discussed in Section 5.4.

We note that the acceleration guidance scheme can be employed in either the analytical form (44)-(45) or the feedback form (46). Use of (44)-(45) yields more accuracy. On the other hand, use of (46) yields more stability.

We also note that, in both the analytical form (44)-(45) and the feedback form (46), the value of the proportionality constant C must be specified. From the analysis of the optimal trajectories (Figs. 5-6), it appears that the most desirable value is

$$C = 0.50. \tag{47}$$

Integrated Form. An integrated form of the acceleration guidance law (39) can be obtained by observing that, if the path inclination is sufficiently small, the hypothesis

$$\cos\gamma \cong 1 \tag{48}$$

can be employed. Hence, (39) becomes

$$\dot{V} + C\dot{W}_x = 0, \tag{49}$$

which upon integration yields

$$V - V_0 + C(W_x - W_{x0}) = 0. \tag{50}$$

This relation can be implemented through the feedback control law

$$\alpha - \tilde{\alpha}(V) = -K[V_0 - V + C(W_{x0} - W_x)], \qquad \alpha \leq \alpha_*, \tag{51}$$

where K is the gain coefficient. The constant C is set at the level (47).

5.4. Implementation of the Guidance Laws. In the previous sections, we presented three guidance schemes: (A) gamma guidance, (B) theta guidance, and (C) acceleration guidance. All of these schemes are based on the measurement of the local values of the state variables, the control variables, and the windshear intensity.

We observe that the values of V, γ, θ, α can be measured with present instrumentation. On the other hand, the value of $\dot{W}_x$ cannot be determined with present instrumentation, but can be computed indirectly from acceleration measurements.

Computation of $\dot{W}_x$. Consider Eq. (1a),

$$\dot{x} = V \cos \gamma + W_x, \tag{52}$$

and observe that its time derivative is given by

$$\ddot{x} = \dot{V} \cos \gamma - V \sin \gamma \dot{\gamma} + \dot{W}_x. \tag{53}$$

For small values of the path inclination, the approximations

$$\cos \gamma \cong 1, \tag{54a}$$

$$\sin \gamma \cong \gamma, \tag{54b}$$

$$|V\gamma\dot{\gamma}| \ll |\dot{V}| \tag{54c}$$

can be employed. As a consequence, Eq. (53) reduces to

$$\dot{W}_x = \ddot{x} - \dot{V}. \tag{55}$$

In turn, $\ddot{x}$ can be obtained from the measurement of the inertial acceleration, while $\dot{V}$ can be obtained by taking the time derivative of the relative velocity.

Elevator Deflection. In the previous sections, the gamma guidance, the theta guidance, and the acceleration guidance were expressed in the feedback control forms (23), (37), (46), (51). This is because the rotational motion of the aircraft is not considered in this paper.

If the rotational motion is considered, the elevator deflection δ_e replaces the angle of attack α as the control. As a consequence, the feedback control laws take the following more practical forms:

$$\delta_e - \tilde{\delta}_e = -K[\gamma - \tilde{\gamma}(\dot{W}_x)], \qquad |\delta_e| \leq \delta_{e*}, \tag{56a}$$

$$\delta_e - \tilde{\delta}_e = -K[\theta - \tilde{\theta}(\dot{W}_x, V)], \qquad |\delta_e| \leq \delta_{e*}, \tag{56b}$$

$$\delta_e - \tilde{\delta}_e = -K[-\dot{V} - C\dot{W}_x \cos \gamma], \qquad |\delta_e| \leq \delta_{e*}, \tag{56c}$$

$$\delta_e - \tilde{\delta}_e = -K[V_0 - V + C(W_{x0} - W_x)], \qquad |\delta_e| \leq \delta_{e*}, \tag{56d}$$

where $\tilde{\delta}_e$ is the nominal elevator deflection and δ_{e*} is the upper bound to the elevator deflection. We note that $\tilde{\delta}_e$ is a function of the state variables, to be suitably defined.

5.5. Numerical Results. The near-optimum guidance schemes (A)-(C) were programmed in FORTRAN IV, and the numerical results were obtained in double-precision arithmetic. Computations were performed at Rice University using an NAS-AS-9000 computer.

The interval of integration was divided into 500 steps. The differential systems were integrated using Hamming's modified predictor-corrector method with a special Runge-Kutta starting procedure.

The gamma guidance [Scheme (A)] was implemented in the form given by Eqs. (23) and (30)-(33), with $K = 10$. The theta guidance [Scheme (B)] was implemented in the form given by Eqs. (37)-(38) and (30)-(33), with $K = 10$. The acceleration guidance [Scheme (C)] was implemented in the form given by Eqs. (44)-(45), with $C = 0.50$.

Several combinations of windshear models and windshear intensities were considered (see Refs. 2-3). With reference to a Boeing B-727 aircraft with three JT8D-17 turbofan engines, the data of Section 9 were employed. In particular, the inital conditions are given by Eqs. (75) and the final time is given by Eq. (77).

Complete numerical results are presented in Figs. 7-12 of Ref. 2. Specifically, Figs. 7-8 refer to Scheme (A); Figs. 9-10 refer to Scheme (B); and Figs. 11-12 refer to Scheme (C). Also, Figs. 7, 9, 11 refer to the effect of the windshear model; and Figs. 8, 10, 12 refer to the effect of the windshear intensity. Each figure contains six parts: the wind velocity W_x; the flight altitude h; the relative velocity V; the relative path inclination γ; the angle of attack α; and the pitch attitude angle θ.

Inspection of the numerical results of Ref. 2 shows that: (i) there is a remarkable qualitative agreement between gamma guidance, theta guidance, and acceleration guidance; and (ii) the near-optimal trajectories arising from the above guidance schemes exhibit an excellent qualitative agreement with the optimal trajectories. This being the case, we compare only the gamma guidance trajectories (Figs. 7-8) with the optimal trajectories (Figs. 5-6).

Effect of the Windshear Model. We refer to the gamma guidance trajectories, in connection with wind velocity difference $\Delta W_x = 80\ \text{ft sec}^{-1}$, windshear intensity $\Delta W_x/\Delta x = 0.020\ \text{sec}^{-1}$. We consider the windshear models WS1, WS2, WS3. We recall that, in model WS1, the windshear starts at $x = 0$ ft; in model WS2, the windshear starts at $x = 700$ ft; in model WS3, the windshear starts at $x = 1{,}700$ ft (see Section 9 for details).

From Figs. 5 and 7, we see that a similarity of behavior exists between the gamma guidance trajectories and the optimal trajectories associated with windshear models WS1, WS2, WS3. In particular, the following points must be noted: (i) for the windshear portion of the flight, the gamma

guidance trajectories are quite close to the optimal trajectories; (ii) for the prewindshear portion of the flight, the gamma guidance trajectories are characterized by constant angle of attack and constant relative velocity; on the other hand, the optimal trajectories tend to decrease slightly the angle of attack, while simultaneously increasing the relative velocity; the difference of behavior is due to the fact that the computation of the gamma guidance trajectories is based on local information, while the computation of the optimal trajectories is based on global information; (iii) for the postwindshear portion of the flight, the gamma guidance trajectories tend to recover the initial value of the path inclination, even though the boundary condition $\gamma(\tau) = \gamma_0$, which was employed in the computation of the optimal trajectories, was not actually imposed in the computation of the gamma guidance trajectories.

Effect of the Windshear Intensity. We refer to the gamma guidance trajectories, in connection with windshear model WS1. We consider the wind velocity differences $\Delta W_x = 80, 100, 120, 140$ ft sec^{-1}, corresponding to the windshear intensities $\Delta W_x/\Delta x = 0.020, 0.025, 0.030, 0.035$ sec^{-1}.

From Figs. 6 and 8, the following points must be noted: (i) for the windshear portion of the flight, the gamma guidance trajectories are quite close to the optimal trajectories; (ii) for the postwindshear portion of the flight, the gamma guidance trajectories tend to recover the initial value of the path inclination, even though the boundary condition $\gamma(\tau) = \gamma_0$, which was employed in the computation of the optimal trajectories, was not actually imposed in the computation of the gamma guidance trajectories; (iii) if the wind velocity difference is $\Delta W_x = 80$ ft sec^{-1}, the altitude distribution has a monotonically climbing behavior in both the gamma guidance trajectory and the optimal trajectory; (iv) if the wind velocity difference is increased to $\Delta W_x = 100$ ft sec^{-1}, the altitude distribution has a monotonically climbing behavior in both the gamma guidance trajectory and the optimal trajectory; (v) if the wind velocity difference is increased to $\Delta W_x = 120$ ft sec^{-1}, the altitude distribution is characterized by a dip in both the gamma guidance trajectory and the optimal trajectory; (vi) if the wind velocity difference is increased to $\Delta W_x = 140$ ft sec^{-1}, both the gamma guidance trajectory and the optimal trajectory hit the ground.

6. Alternative Guidance Schemes

This section pertains to alternative guidance schemes, more specifically: (D) constant alpha guidance; (E) constant velocity guidance; (F) constant

theta guidance; (G) constant relative path inclination guidance; (H) constant absolute path inclination guidance; and (I) linear altitude distribution guidance. The description of the alternative guidance schemes is given in Section 6.1. Then, the numerical results for the alternative guidance schemes are given in Section 6.2, with particular reference to the effect of the windshear intensity.

6.1. Analytical Description. For the sake of completeness, some alternative guidance schemes have been investigated (Ref. 3). Among them, we mention the schemes below.

Constant Alpha Guidance. Scheme (D). Trajectories $\alpha = \text{const}$ have been computed for two values of the angle of attack, namely,

$$\alpha = \alpha_0, \tag{57a}$$

$$\alpha = \alpha_*. \tag{57b}$$

Constant Velocity Guidance. Scheme (E). Trajectories $V = V_0$ have been implemented through the feedback control law

$$\alpha - \alpha_0 = -K(V_0 - V), \qquad \alpha \leq \alpha_*. \tag{58}$$

Constant Theta Guidance. Scheme (F). Trajectories $\theta = \text{const}$ have been computed using the angle of attack program (Ref. 14)

$$\alpha = \theta_0 - \gamma, \qquad \alpha \leq \alpha_*. \tag{59}$$

Alternatively, (59) can be implemented through the feedback control law

$$\alpha - \alpha_0 = -K(\theta - \theta_0), \qquad \alpha \leq \alpha_*. \tag{60}$$

Constant Relative Path Inclination Guidance. Scheme (G). Trajectories $\gamma = \gamma_0$ have been implemented through the feedback control law

$$\alpha - \alpha_0 = -K(\gamma - \gamma_0), \qquad \alpha \leq \alpha_*. \tag{61}$$

Constant Absolute Path Inclination Guidance. Scheme (H). Trajectories $\gamma_e = \gamma_{e0}$ have been implemented through the feedback control law

$$\alpha - \alpha_0 = -K(\gamma_e - \gamma_{e0}), \qquad \alpha \leq \alpha_*. \tag{62}$$

Linear Altitude Distribution Guidance. Scheme (I). Trajectories along which the altitude has a linear distribution,

$$h = h_L(x) = h_0 + (\tan \gamma_{e0})x, \tag{63}$$

have been implemented through the feedback control law

$$\alpha - \alpha_0 = -K[h - h_L(x)] = -K[h - h_0 - (\tan \gamma_{e0})x], \qquad \alpha \leq \alpha_*. \tag{64}$$

6.2. Numerical Results. The alternative guidance schemes (D)–(I) were programmed in FORTRAN IV, and the numerical results were obtained in double-precision arithmetic. Computations were performed at Rice University using an NAS-AS-9000 computer.

The interval of integration was divided into 500 steps. The differential systems were integrated using Hamming's modified predictor-corrector method with a special Runge–Kutta starting procedure.

Several combinations of windshear models and windshear intensities were considered (see Ref. 3). With reference to a Boeing B-727 aircraft with three JT8D-17 turbofan engines, the data of Section 9 were employed. In particular, the initial conditions are given by Eqs. (75) and the final time is given by Eq. (77).

The numerical results show that guidance schemes (D)–(I) are inferior to guidance schemes (A)–(C) for a variety of technical reasons. In particular, for the case where the wind velocity difference is $\Delta W_x = 120$ ft sec^{-1} and the windshear intensity is $\Delta W_x/\Delta x = 0.030$ sec^{-1}, it is shown that the trajectories associated with guidance schemes (D)–(I) hit the ground, while the trajectories associated with guidance schemes (A)–(C) clear the ground. The details can be found in Ref. 3 and are omitted here, for the sake of brevity.

7. Comparison of the Guidance Schemes

In Sections 4–6, we presented optimal trajectories, near-optimum guidance schemes, and alternative guidance schemes, with the following understanding: the computation of the optimal trajectories of Section 4 is based on global information on the wind flow field and the state of the aircraft; the computation of trajectories using the near-optimum guidance schemes (A)–(C) of Section 5 is based on local information on the wind flow field and the state of the aircraft; and the computation of trajectories using the alternative guidance schemes (D)–(I) of Section 6 is based on local information on the state of the aircraft.

A comparison of the guidance schemes is presented in Tables 4–5 in terms of two performance indexes,

$$M = \max_t |\gamma(t) - \gamma(0)|, \qquad 0 \leq t \leq \tau, \tag{65a}$$

$$N = |\gamma(\tau) - \gamma(0)|. \tag{65b}$$

Clearly, (65a) represents the maximum deviation of the path inclination from the reference value, and (65b) represents the final deviation of the path inclination from the reference value.

Table 4. Comparison of guidance schemes: Values of $M = \max_t |\gamma - \gamma_0|$.

Symbol	Guidance scheme	Remark	$\Delta W_x = 80$	$\Delta W_x = 100$	$\Delta W_x = 120$	$\Delta W_x = 140$
(P7)	Optimal trajectory	—	4.02	6.62	8.58	11.10(*)
(A)	Gamma guidance	$K = 10$	4.72	6.81	10.82	15.96(*)
(B)	Theta guidance	$K = 10$	4.51	8.54	13.01	17.76(*)
(C)	Acceleration guidance	$C = 0.50$	5.19	7.29	10.90	14.94(*)
(D)	Constant alpha guidance $\alpha = \alpha_0$	$K = 10$	16.38(*)	20.27(*)	24.07(*)	27.79(*)
(D)	Constant alpha guidance $\alpha = \alpha_*$	$K = 10$	23.69	26.88(*)	30.01(*)	32.91(*)
(E)	Constant velocity guidance $V = V_0$	$K = 10$	14.36(*)	17.55(*)	20.47(*)	23.11(*)
(F)	Constant theta guidance $\theta = \theta_0$	$K = 10$	7.43	12.18	16.95(*)	21.49(*)
(G)	Constant relative path inclination guidance $\gamma = \gamma_0$	$K = 10$	10.84	15.87	20.51(*)	24.86(*)
(H)	Constant absolute path inclination guidance $\gamma_e = \gamma_{e0}$	$K = 10$	12.47	17.38	21.93(*)	26.22(*)
(I)	Linear altitude distribution guidance $\tan \gamma_e = \tan \gamma_{e0}$	$K = 10$	12.44	17.25	21.82(*)	26.14(*)

Values of M are in degrees. Values of ΔW_x are in ft sec^{-1}. Asterisk denotes crash.

The computational results show that the guidance schemes (D)-(I) are inferior to the guidance schemes (A)-(C), which in turn yield trajectories which are quite close to the optimal trajectories. In particular, for the case where the wind velocity difference is $\Delta W_x = 120$ ft sec^{-1} and the windshear intensity is $\Delta W_x / \Delta x = 0.030$ sec^{-1}, the trajectories arising from the alternative guidance schemes (D)-(I) hit the ground, while the trajectories arising from the near-optimum guidance schemes (A)-(C) clear the ground, just as the optimal trajectories.

Table 5. Comparison of guidance schemes: Values of $N = |\gamma(\tau) - \gamma(0)|$.

Symbol	Guidance scheme	Remark	$\Delta W_x = 80$	$\Delta W_x = 100$	$\Delta W_x = 120$	$\Delta W_x = 140$
(P7)	Optimal trajectory	—	0.00	0.00	0.00	0.00(*)
(A)	Gamma guidance	$K = 10$	0.02	0.01	0.01	0.01(*)
(B)	Theta guidance	$K = 10$	0.14	0.09	0.08	0.07(*)
(C)	Acceleration guidance	$C = 0.50$	0.34	0.19	0.06	0.01(*)
(D)	Constant alpha guidance $\alpha = \alpha_0$	$K = 10$	14.58(*)	17.83(*)	20.82(*)	23.48(*)
(D)	Constant alpha guidance $\alpha = \alpha_*$	$K = 10$	17.22	20.24(*)	22.65(*)	24.84(*)
(E)	Constant velocity guidance $V = V_0$	$K = 10$	0.79(*)	1.18(*)	1.94(*)	2.63(*)
(F)	Constant theta guidance $\theta = \theta_0$	$K = 10$	1.34	0.73	0.00(*)	0.67(*)
(G)	Constant relative path inclination guidance $\gamma = \gamma_0$	$K = 10$	0.17	0.05	0.04(*)	0.11(*)
(H)	Constant absolute path inclination guidance $\gamma_e = \gamma_{e0}$	$K = 10$	2.20	3.00	3.83(*)	4.72(*)
(I)	Linear altitude distribution guidance $\tan \gamma_e = \tan \gamma_{e0}$	$K = 10$	8.58	12.60	16.28(*)	19.63(*)

Values of N are in degrees. Values of ΔW_x are in ft sec^{-1}. Asterisk denotes crash.

From the present analysis and from the analyses of Refs. 1-3, the following concepts emerge.

(i) In a windshear, the relative path inclination should be such that the two-sided inequality $0 \leq \gamma \leq \gamma_0$ is satisfied, if at all possible. Violation of the upper bound is not desirable, because it might cause excessive velocity loss. Conversely, violation of the lower bound is not desirable, because of the ensuing altitude loss.

(ii) In a windshear, the value of the relative path inclination should be adjusted to the windshear intensity, in the following sense: as the windshear intensity increases, lower values of γ become desirable, so as to slow down the magnitude of the velocity drop.

Properties (i)-(ii) are better reflected in the guidance schemes (A)-(C) than in the guidance schemes (D)-(I). Hence, the trajectories arising from the guidance schemes (A)-(C) are closer to the optimal trajectories than the trajectories arising from the guidance schemes (D)-(I).

8. Conclusions

This paper is concerned with guidance strategies for near-optimum performance in a windshear. This is a wind characterized by sharp change in intensity and direction over a relatively small region of space. The take-off problem is considered with reference to flight in a vertical plane.

First, trajectories for optimum performance in a windshear are determined for different windshear models and different windshear intensities. Use is made of the methods of optimal control theory in conjunction with the dual sequential gradient-restoration algorithm (DSGRA) for optimal control problems. In this approach, global information on the wind flow field is needed.

Then, guidance strategies for near-optimum performance in a windshear are developed, starting from the optimal trajectories. Specifically, three guidance schemes are presented: (A) gamma guidance, based on the relative path inclination; (B) theta guidance, based on the pitch attitude angle; and (C) acceleration guidance, based on the relative acceleration. In this approach, local information on the wind flow field is needed.

Next, several alternative schemes are investigated for the sake of completeness, more specifically: (D) constant alpha guidance; (E) constant velocity guidance; (F) constant theta guidance; (G) constant relative path inclination guidance; (H) constant absolute path inclination guidance; and (I) linear altitude distribution guidance.

Numerical experiments show that guidance schemes (A)-(C) produce trajectories which are quite close to the optimum trajectories. In addition, the near-optimum trajectories associated with guidance schemes (A)-(C) are considerably superior to the trajectories arising from the alternative guidance schemes (D)-(I).

An important characteristic of guidance schemes (A)-(C) is their simplicity. Indeed, these guidance schemes are implementable using available instrumentation and/or modification of available instrumentation.

In subsequent papers, the analysis presented here for take-off trajectories will be extended to include (i) rotational motion effects and (ii) a more complete windshear model. In particular, for downdraft effects, see Refs. 41-42. Also in subsequent papers, the treatment developed for take-off trajectories will be extended to include landing trajectories.

9. Appendix: Data for the Examples

In this appendix, we present the data used in the numerical experiments. The airplane under consideration is a Boeing B-727 aircraft with three JT8D-17 turbofan engines. It is assumed that the aircraft has become airborne from a runway located at sea-level altitude. It is also assumed that the ambient temperature is 100 deg Fahrenheit.

Thrust. It is assumed that the engines are operating at maximum power setting. The dependence of the thrust on the altitude is disregarded, and the thrust is assumed to depend on the velocity only. At $h = 0$ ft, the thrust is represented by Eq. (4), with

$$A_0 = \ 0.4456\ E+05 \text{ lb}, \qquad 0 \leq V \leq 422 \text{ ft sec}^{-1}, \tag{66a}$$

$$A_1 = -0.2398\ E+02 \text{ lb ft}^{-1} \text{ sec}, \qquad 0 \leq V \leq 422 \text{ ft sec}^{-1}, \tag{66b}$$

$$A_2 = \ 0.1442\ E-01 \text{ lb ft}^{-2} \text{ sec}^2, \qquad 0 \leq V \leq 422 \text{ ft sec}^{-1}. \tag{66c}$$

The inclination of the thrust with respect to the aircraft reference line is assumed to be

$$\delta = 0.2000\ E+01 \text{ deg}. \tag{67}$$

Drag. The dependence of the density on the altitude is disregarded, and the drag is assumed to depend on the velocity and the angle of attack only. This function is represented by Eqs. (5)-(6), with[7]

$$\rho = 0.2203\ E-02 \text{ lb ft}^{-4} \text{ sec}^2, \tag{68a}$$

$$S = 0.1560\ E+04 \text{ ft}^2, \tag{68b}$$

and

$$B_0 = \ 0.7351\ E-01, \qquad 0 \leq \alpha \leq 16 \text{ deg}, \tag{69a}$$

$$B_1 = -0.8617\ E-01, \qquad 0 \leq \alpha \leq 16 \text{ deg}, \tag{69b}$$

$$B_2 = \ 0.1996\ E+01, \qquad 0 \leq \alpha \leq 16 \text{ deg}. \tag{69c}$$

[7] The aerodynamic data refer to gear up and flap setting $\delta_F = 15$ deg.

Lift. Like the drag, the lift is assumed to depend on the velocity and the angle of attack only. This function is represented by Eqs. (7)-(8), with ρ, S given by Eqs. (68) and

$$C_0 = 0.1667\ E+00, \qquad 0 \leq \alpha \leq 16 \text{ deg}, \tag{70a}$$

$$C_1 = 0.6231\ E+01, \qquad 0 \leq \alpha \leq 16 \text{ deg}, \tag{70b}$$

$$C_2 = -0.2165\ E+02, \qquad 12 \leq \alpha \leq 16 \text{ deg}. \tag{70c}$$

Weight. The weight of the aircraft is assumed to be constant, specifically,

$$W = 0.1800\ E+06 \text{ lb}. \tag{71}$$

Windshear. The assumed wind model involves the transition from a uniform headwind to a uniform tailwind. Therefore, it is governed by the three-parameter family (11), in which the parameter a is associated with the windshear onset, the parameter b is associated with the windshear termination, and the parameter k is associated with the wind velocity difference ΔW_x and the windshear intensity $\Delta W_x/\Delta x$ (for given values of a and b).

Three particular models are considered. In windshear model WS1, the constants a, b are given by

$$a = 0.3000\ E+03 \text{ ft}, \qquad b = 0.4300\ E+04 \text{ ft}. \tag{72a}$$

In windshear model WS2, the constants a, b are given by

$$a = 0.1000\ E+04 \text{ ft}, \qquad b = 0.5000\ E+04 \text{ ft}. \tag{72b}$$

In windshear model WS3, the constants a, b are given by

$$a = 0.2000\ E+04 \text{ ft}, \qquad b = 0.6000\ E+04 \text{ ft}. \tag{72c}$$

It must be noted that the windshear models WS1, WS2, WS3 involve corners, which are smoothed using the technique discussed in Ref. 1. Each smoothing interval is assumed to be 600 ft in length and is centered around the respective corner.

It must also be noted that the windshear models WS1, WS2, WS3 are characterized by the same transition length $b-a = 4{,}000$ ft. Hence, Table 1 supplies the relation between the parameter k, the wind velocity difference ΔW_x, and the windshear intensity $\Delta W_x/\Delta x$.

Inequality Constraints. The angle of attack is subject to Ineq. (13), with

$$\alpha_* = 0.1600\ E+02 \text{ deg}. \tag{73}$$

The time derivative of the angle of attack is subject to the Ineq. (14), with

$$C = 0.3000\ E+01 \text{ deg sec}^{-1}. \tag{74}$$

Initial Conditions. The following initial conditions are assumed:

$$x(0) = 0.0000\ E+00 \text{ ft}, \tag{75a}$$

$$h(0) = 0.5000\ E+02 \text{ ft}, \tag{75b}$$

$$V(0) = 0.2768\ E+03 \text{ ft sec}^{-1}, \tag{75c}$$

$$\gamma(0) = 0.6989\ E+01 \text{ deg}, \tag{75d}$$

and

$$\alpha(0) = 0.1036\ E+02 \text{ deg}. \tag{76}$$

Note that the velocity (75c) is FAA certification velocity V_2, augmented by 10 knots. In turn, the velocity V_2+10 (in knots) corresponds approximately to the steepest climb condition in quasi-steady flight.

Final Time. The final time is set at the value

$$\tau = 0.4000\ E+02 \text{ sec}. \tag{77}$$

This is about twice the duration of the windshear encounter (18 sec).

Final Conditions. In boundary condition model BC1, it is required that

$$\gamma(\tau) = 0.6989\ E+01 \text{ deg}. \tag{78}$$

Remark. For the optimal trajectories of Section 4, use is made of (75)-(78). For the guidance schemes of Sections 5-6, use is made of (75) and (77), while (76) and (78) are disregarded.

Special Constants. For the optimal trajectories of Section 4, the numerical constants appearing in the performance indexes I and J of Problem (P7) are given by

$$\gamma_R = 0.6989\ E+01 \text{ deg}, \tag{79a}$$

$$q = 6. \tag{79b}$$

For the near-optimum guidance schemes of Section 5, the gain coefficient K is set at the level

$$K = 10. \tag{80}$$

In particular, the constant C of the acceleration guidance scheme is set at the level

$$C = 0.50. \tag{81}$$

Finally, for the alternative guidance schemes of Section 6, the gain coefficient K is set at the level

$$K = 10. \tag{82}$$

References

1. MIELE, A., WANG, T., and MELVIN, W. W., *Optimal Take-Off Trajectories in the Presence of Windshear*, Journal of Optimization Theory and Applications, Vol. 49, No. 1, pp. 1–45, 1986.
2. MIELE, A., WANG, T., and MELVIN, W. W., *Guidance Strategies for Near-Optimum Performance in a Windshear, Part 1, Take-Off, Basic Strategies*, Rice University, Aero-Astronautics Report No. 201, 1986.
3. MIELE, A., WANG, T., and MELVIN, W. W., *Guidance Strategies for Near-Optimum Performance in a Windshear, Part 2, Take-Off, Comparison Strategies*, Rice University, Aero-Astronautics Report No. 202, 1986.
4. ANONYMOUS, N. N., *Low Altitude Windshear and Its Hazard to Aviation*, National Academy Press, Washington, DC, 1983.
5. MIELE, A., *Flight Mechanics, Vol. 1, Theory of Flight Paths*, Addison-Wesley Publishing Company, Reading, Massachusetts, 1962.
6. FROST, W., and CROSBY, B., *Investigations of Simulated Aircraft Flight through Thunderstorm Outflows*, NASA, Contractor Report No. 3052, 1978.
7. MCCARTHY, J., BLICK, E. F., and BENSCH, R. R., *Jet Transport Performance in Thunderstorm Windshear Conditions*, NASA, Contractor Report No. 3207, 1979.
8. PSIAKI, M. L., and STENGEL, R. F., *Analysis of Aircraft Control Strategies for Microburst Encounter*, Paper No. AIAA-84-0238, AIAA 22nd Aerospace Sciences Meeting, Reno, Nevada, 1984.
9. FROST, W., and BOWLES, R. L., *Windshear Terms in the Equations of Aircraft Motion*, Journal of Aircraft, Vol. 21, No. 11, pp. 866–872, 1984.
10. ZHU, S. X., and ETKIN, B., *Fluid-Dynamic Model of a Downburst*, University of Toronto, Institute for Aerospace Studies, Report No. UTIAS-271, 1983.
11. ALEXANDER, M. B., and CAMP, D. W., *Wind Speed and Direction Shears with Associated Vertical Motion during Strong Surface Winds*, NASA, Technical Memorandum No. 82566, 1984.
12. FROST, W., CHANG, H. P., ELMORE, K. L., and MCCARTHY, J., *Simulated Flight through JAWS Windshear: In-Depth Analysis Results*, Paper No. AIAA-84-0276, AIAA 22nd Aerospace Sciences Meeting, Reno, Nevada, 1984.
13. CAMPBELL, C. W., *A Spatial Model of Windshear and Turbulence for Flight Simulation*, NASA, Technical Paper No. 2313, 1984.
14. ANONYMOUS, N. N., *Flight Path Control in Windshear*, Boeing Airliner, pp. 1–12, January–March 1985.
15. LEITMANN, G., *The Calculus of Variations and Optimal Control*, Plenum Publishing Corporation, New York, New York, 1981.
16. MIELE, A., PRITCHARD, R. E., and DAMOULAKIS, J. N., *Sequential Gradient-Restoration Algorithm for Optimal Control Problems*, Journal of Optimization Theory and Applications, Vol. 5, No. 4, pp. 235–282, 1970.
17. MIELE, A., DAMOULAKIS, J. N., CLOUTIER, J. R., and TIETZE, J. L., *Sequential Gradient-Restoration Algorithm for Optimal Control Problems with Nondifferential Constraints*, Journal of Optimization Theory and Applications, Vol. 13, No. 2, pp. 218–255, 1974.

18. MIELE, A., *Recent Advances in Gradient Algorithms for Optimal Control Problems*, Jc urnal of Optimization Theory and Applications, Vol. 17, Nos. 5/6, pp. 361-430, 1975.
19. GONZALEZ, S., and MIELE, A., *Sequential Gradient-Restoration Algorithm for Optimal Control Problems with General Boundary Conditions*, Journal of Optimization Theory and Applications, Vol. 26, No. 3, pp. 395-425, 1978.
20. MIELE, A., *Gradient Algorithms for the Optimization of Dynamic Systems*, Control and Dynamic Systems, Advances in Theory and Application, Edited by C. T. Leondes, Academic Press, New York, New York, Vol. 16, pp. 1-52, 1980.
21. MIELE, A., and WANG, T., *Primal-Dual Properties of Sequential Gradient-Restoration Algorithms for Optimal Control Problems, Part 1: Basic Problem*, Rice University, Aero-Astronautics Report No. 183, 1985.
22. MIELE, A., and WANG, T., *Primal-Dual Properties of Sequential Gradient-Restoration Algorithms for Optimal Control Problems, Part 2: General Problem*, Rice University, Aero-Astronautics Report No. 184, 1985.
23. JOHNSON, C. D., *Optimal Control with Chebyshev Minimax Performance Index*, Journal of Basic Engineering, Vol. 89, No. 2, pp. 251-262, 1967.
24. MICHAEL, G. J., *Computation of Chebyshev Optimal Control*, AIAA Journal, Vol. 9, No. 5, pp. 973-975, 1971.
25. WARGA, J., *Minimax Problems and Unilateral Curves in the Calculus of Variations*, SIAM Journal on Control, Vol. 3, No. 1, pp. 91-105, 1965.
26. POWERS, W. F., *A Chebyshev Minimax Technique Oriented to Aerospace Trajectory Optimization Problems*, AIAA Journal, Vol. 10, No. 10, pp. 1291-1296, 1972.
27. HOLMAKER, K., *A Minimax Optimal Control Problem*, Journal of Optimization Theory and Applications, Vol. 28, No. 3, pp. 391-410, 1979.
28. HOLMAKER, K., *A Property of an Autonomous Minimax Optimal Control Problem*, Journal of Optimization Theory and Applications, Vol. 32, No. 1, pp. 81-87, 1980.
29. MIELE, A., MOHANTY, B. P., VENKATARAMAN, P., and KUO, Y. M., *Numerical Solution of Minimax Problems of Optimal Control, Part 1*, Journal of Optimization Theory and Applications, Vol. 38, No. 1, pp. 97-109, 1982.
30. MIELE, A., MOHANTY, B. P., VENKATARAMAN, P., and KUO, Y. M., *Numerical Solution of Minimax Problems of Optimal Control, Part 2*, Journal of Optimization Theory and Applications, Vol. 38, No. 1, pp. 111-135, 1982.
31. MIELE, A., and VENKATARAMAN, P., *Optimal Trajectories for Aeroassisted Orbital Transfer*, Acta Astronautica, Vol. 11, Nos. 7/8, pp. 423-433, 1984.
32. MIELE, A., and VENKATARAMAN, P., *Minimax Optimal Control and Its Application to the Reentry of a Space Glider*, Recent Advances in the Aerospace Sciences, Edited by L. Casci, Plenum Publishing Corporation, New York, New York, pp. 21-40, 1985.
33. MIELE, A., and BASAPUR, V. K., *Approximate Solutions to Minimax Optimal Control Problems for Aeroassisted Orbital Transfer*, Acta Astronautica, Vol. 12, No. 10, pp. 809-818, 1985.
34. MIELE, A., BASAPUR, V. K., and MEASE, K. D., *Nearly-Grazing Optimal Trajectories for Aeroassisted Orbital Transfer*, Journal of the Astronautical Sciences, Vol. 34, No. 1, pp. 3-18, 1986.

35. MIELE, A., and WANG, T., *An Elementary Proof of a Functional Analysis Result Having Interest for Minimax Optimal Control of Aeroassisted Orbital Transfer Vehicles*, Rice University, Aero-Astronautics Report No. 182, 1985.
36. COTTRELL, R. G., *Optimal Intercept Guidance for Short-Range Tactical Missiles*, AIAA Journal, Vol. 9, No. 7, pp. 1414–1415, 1971.
37. ASHER, R. B., and MATUZEWSKI, J. P., *Optimal Guidance for Maneuvering Targets*, Journal of Spacecraft and Rockets, Vol. 11, No. 3, pp. 204–206, 1974.
38. STENGEL, R. F., *Optimal Guidance for the Space Shuttle Transition*, Journal of Spacecraft and Rockets, Vol. 11, No. 3, pp. 173–179, 1974.
39. NAZAROFF, G. J., *An Optimal Terminal Guidance Law*, IEEE Transactions on Automatic Control, Vol. AC-21, No. 3, pp. 407–408, 1976.
40. GUELMAN, N., and SHINAR, J., *Optimal Guidance Law in the Plane*, Journal of Guidance, Control, and Dynamics, Vol. 7, No. 4, pp. 471–476, 1984.
41. MIELE, A., WANG, T., and MELVIN, W. W., *Optimization and Acceleration Guidance of Flight Trajectories in a Windshear*, Paper No. AIAA-86-2036-CP, AIAA Guidance, Navigation, and Control Conference, Williamsburg, Virginia, 1986.
42. MIELE, A., WANG, T., and MELVIN, W. W., *Optimization and Gamma/Theta Guidance of Flight Trajectories in a Windshear*, Paper No. ICAS-86-564, 15th Congress of the International Council of the Aeronautical Sciences, London, England, 1986.

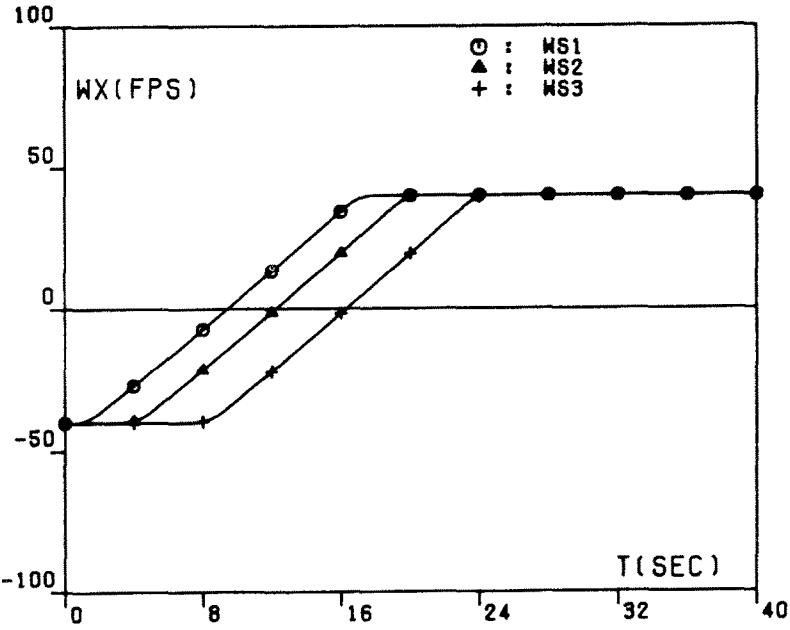

Fig. 5A. Horizontal component of the wind velocity W_x versus time t (optimal trajectory, effect of the windshear model).

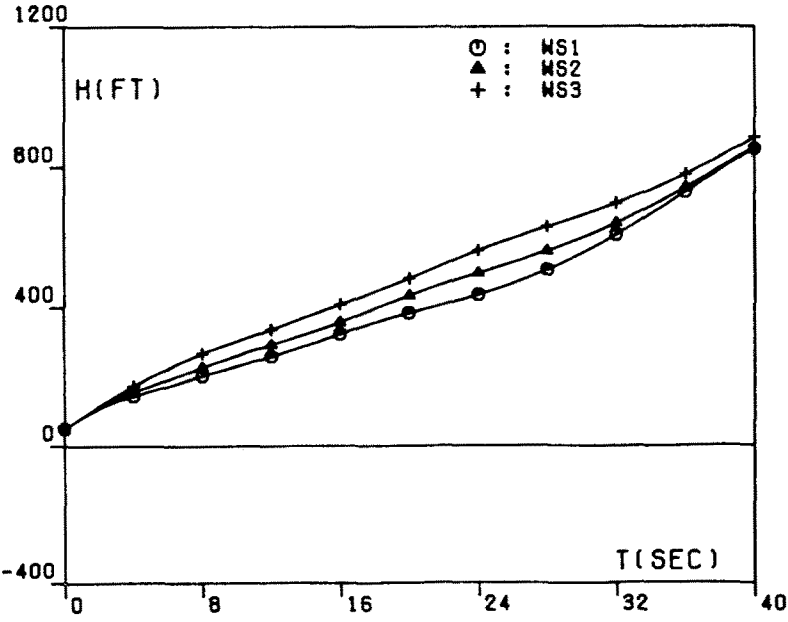

Fig. 5B. Altitude h versus time t (optimal trajectory, effect of the windshear model).

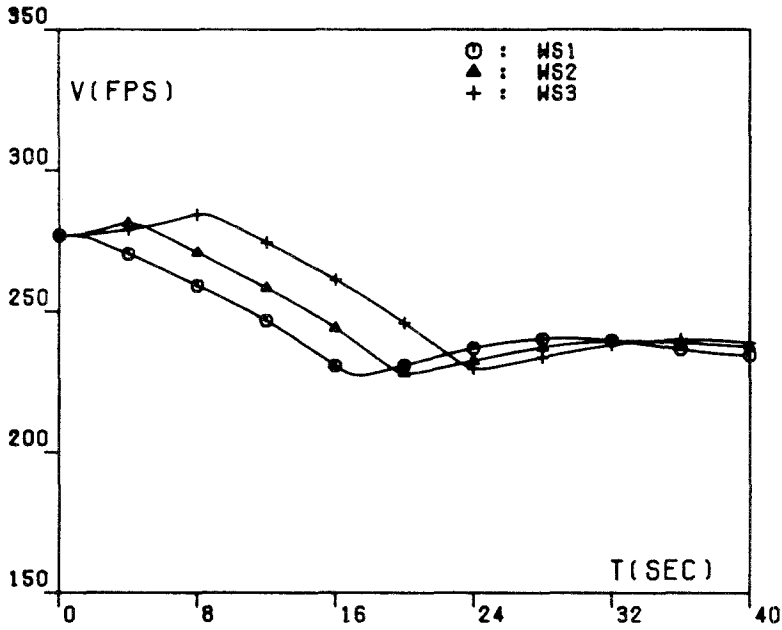

Fig. 5C. Relative velocity V versus time t (optimal trajectory, effect of the windshear model).

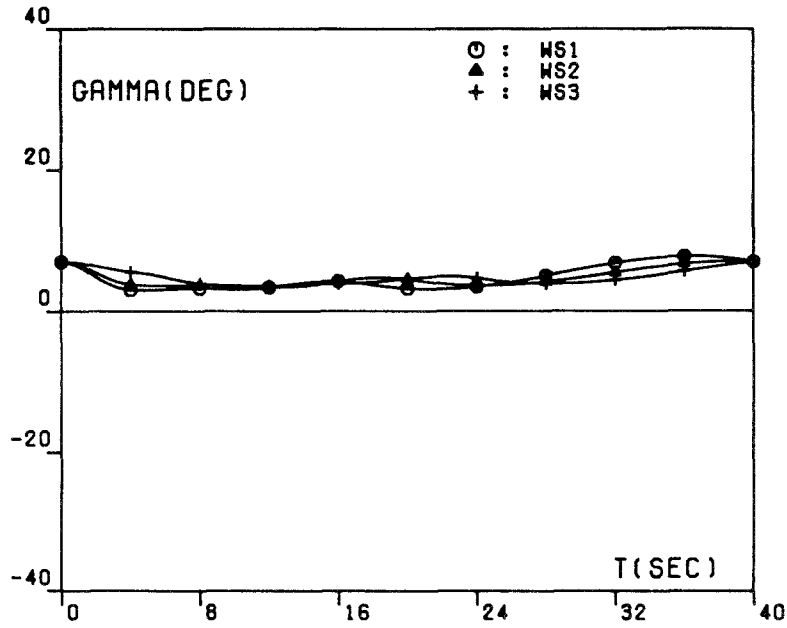

Fig. 5D. Relative path inclination γ versus time t (optimal trajectory, effect of the windshear model).

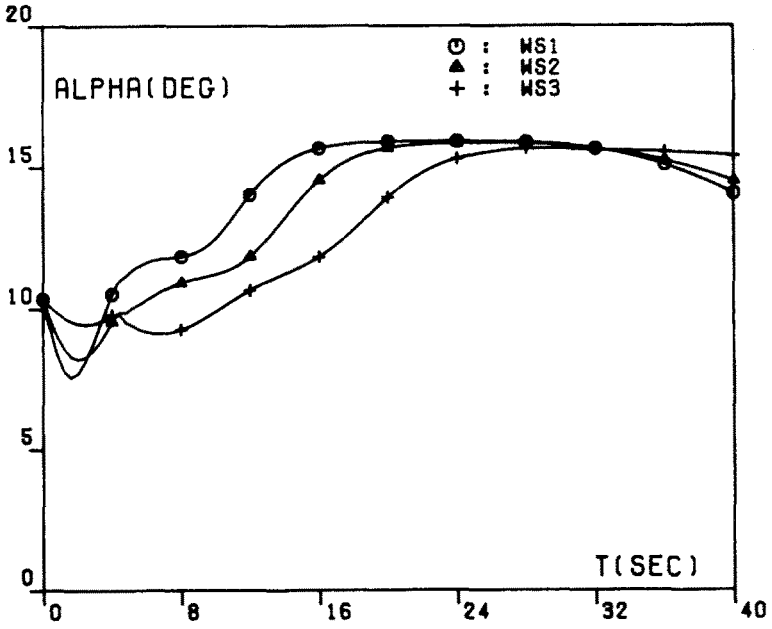

Fig. 5E. Relative angle of attack α versus time t (optimal trajectory, effect of the windshear model).

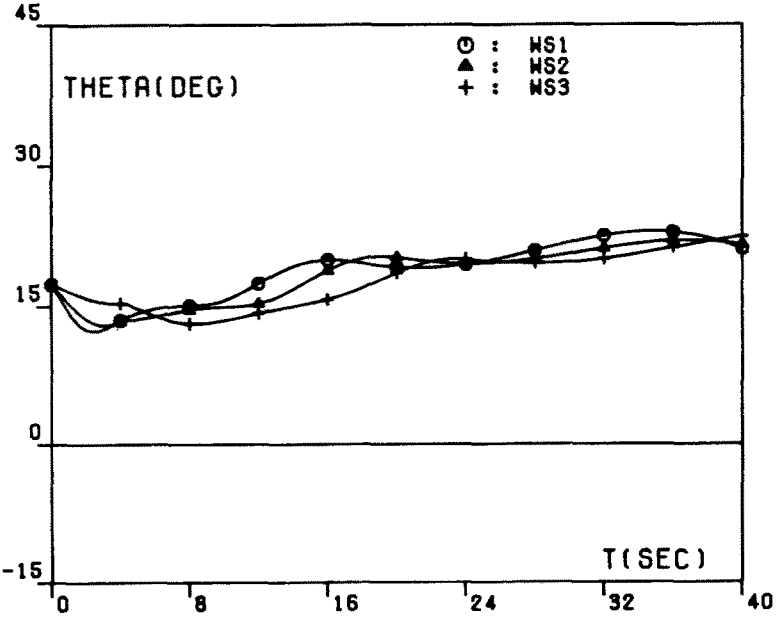

Fig. 5F. Pitch attitude angle θ versus time t (optimal trajectory, effect of the windshear model).

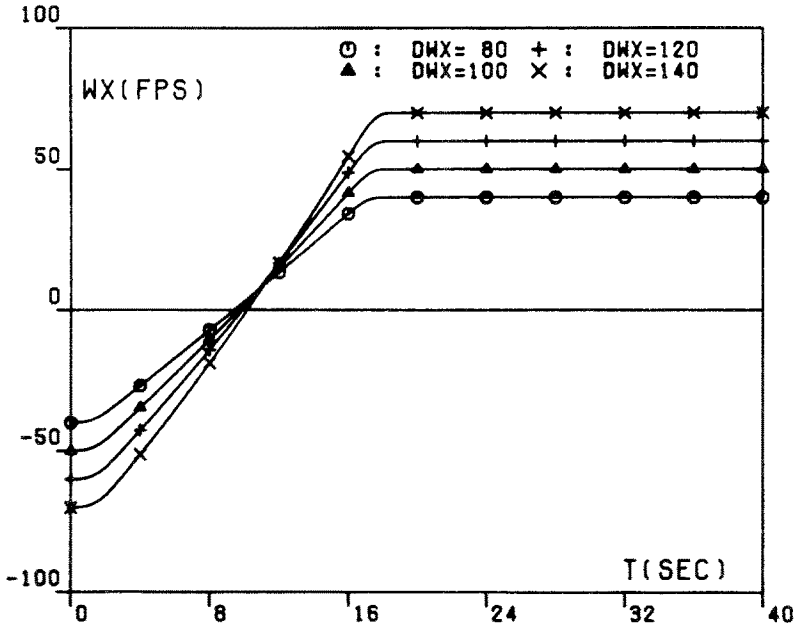

Fig. 6A. Horizontal component of the wind velocity W_x versus time t (optimal trajectory, effect of the windshear intensity).

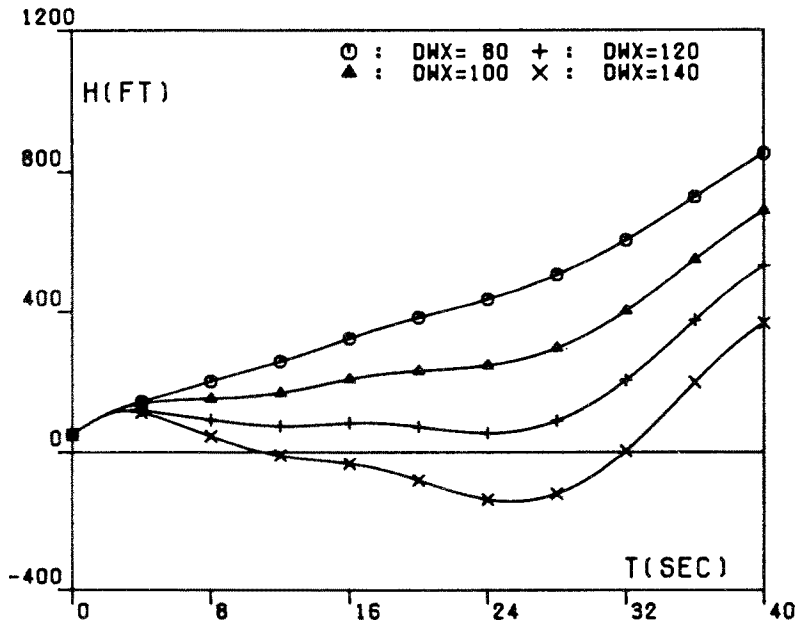

Fig. 6B. Altitude h versus time t (optimal trajectory, effect of the windshear intensity).

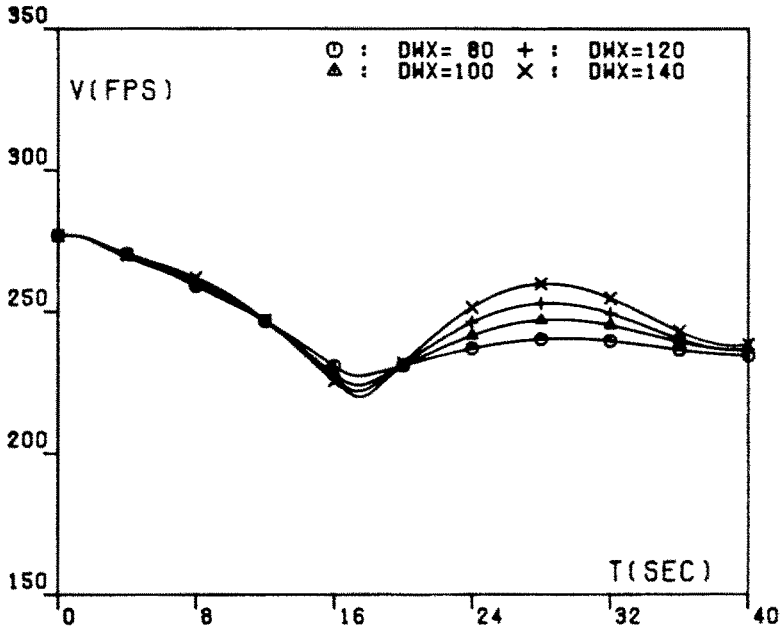

Fig. 6C. Relative velocity V versus time t (optimal trajectory, effect of the windshear intensity).

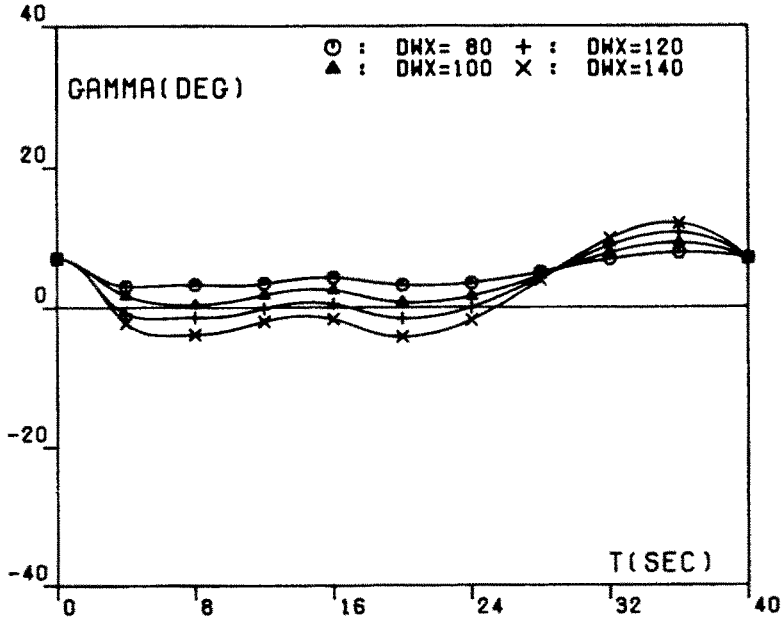

Fig. 6D. Relative path inclination γ versus time t (optimal trajectory, effect of the windshear intensity).

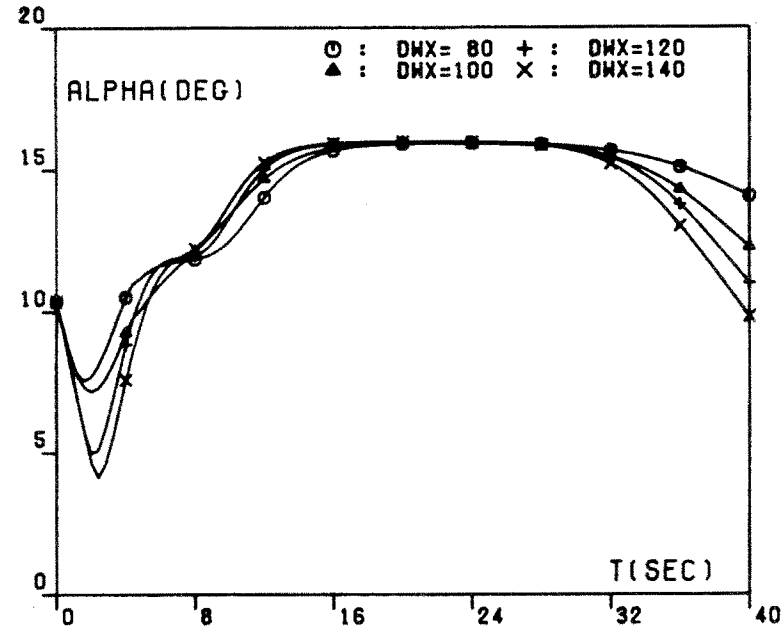

Fig. 6E. Relative angle of attack α versus time t (optimal trajectory, effect of the windshear intensity).

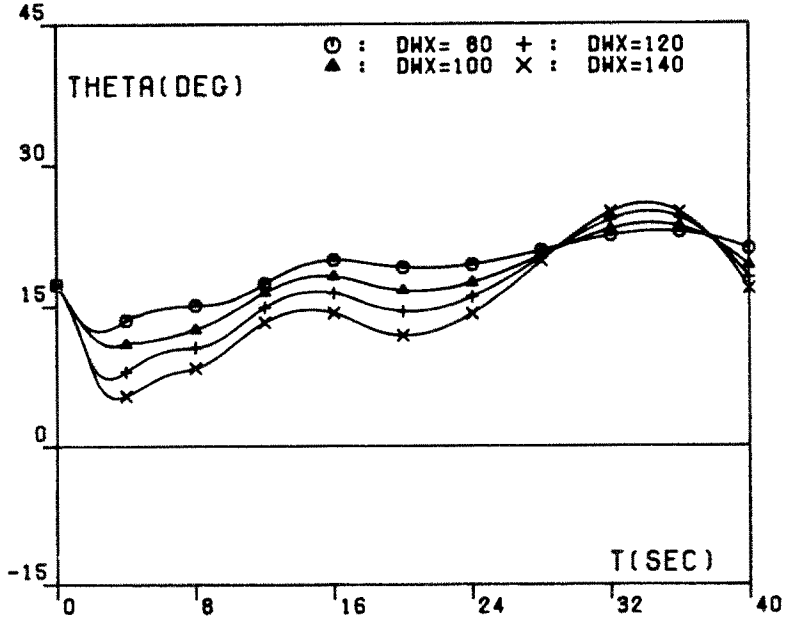

Fig. 6F. Pitch attitude angle θ versus time t (optimal trajectory, effect of the windshear intensity).

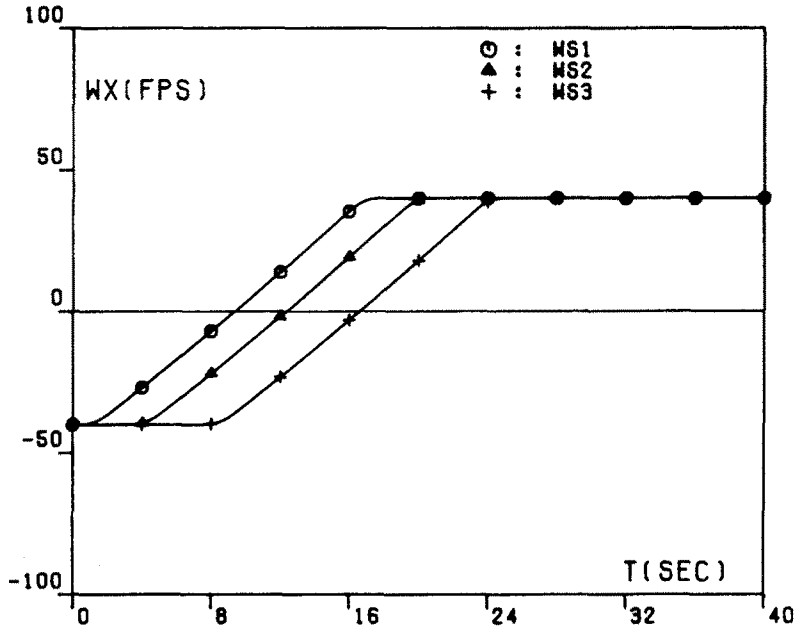

Fig. 7A. Horizontal component of the wind velocity W_x versus time t (gamma guidance, effect of the windshear model).

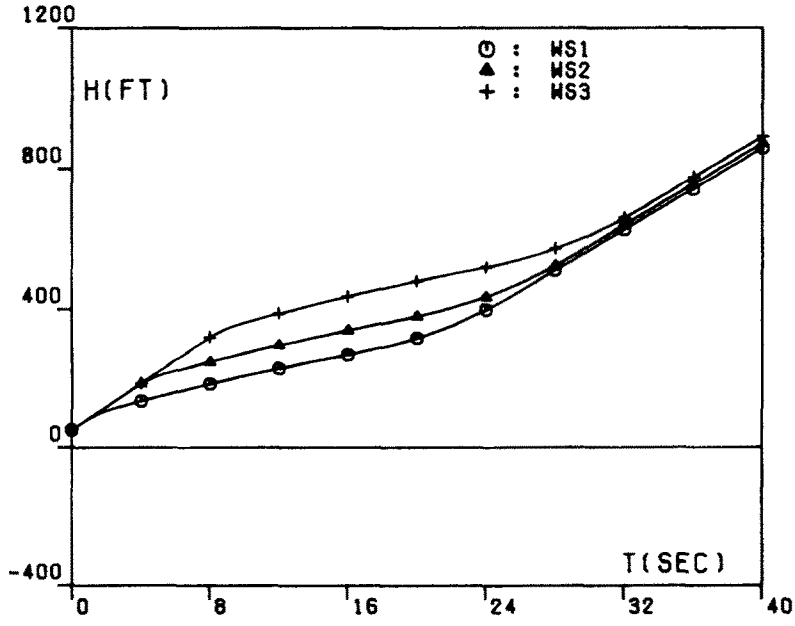

Fig. 7B. Altitude h versus time t (gamma guidance, effect of the windshear model).

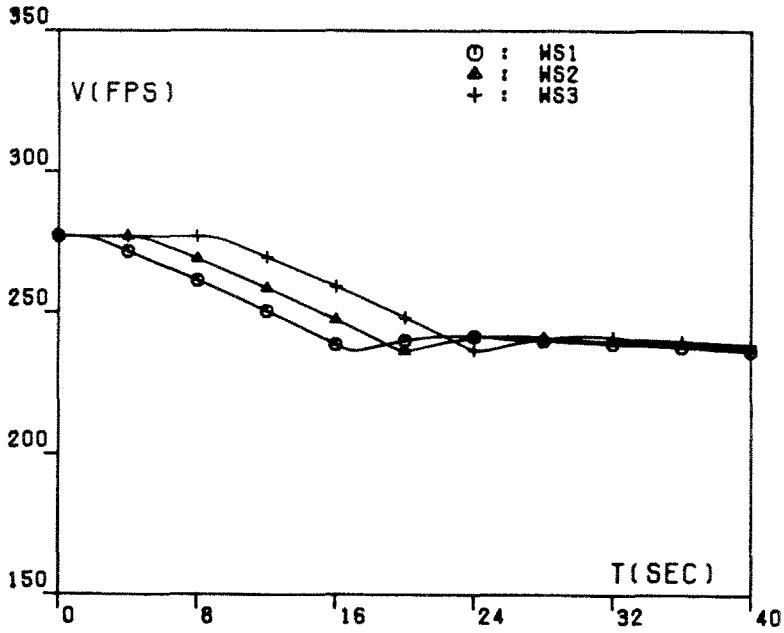

Fig. 7C. Relative velocity V versus time t (gamma guidance, effect of the windshear model).

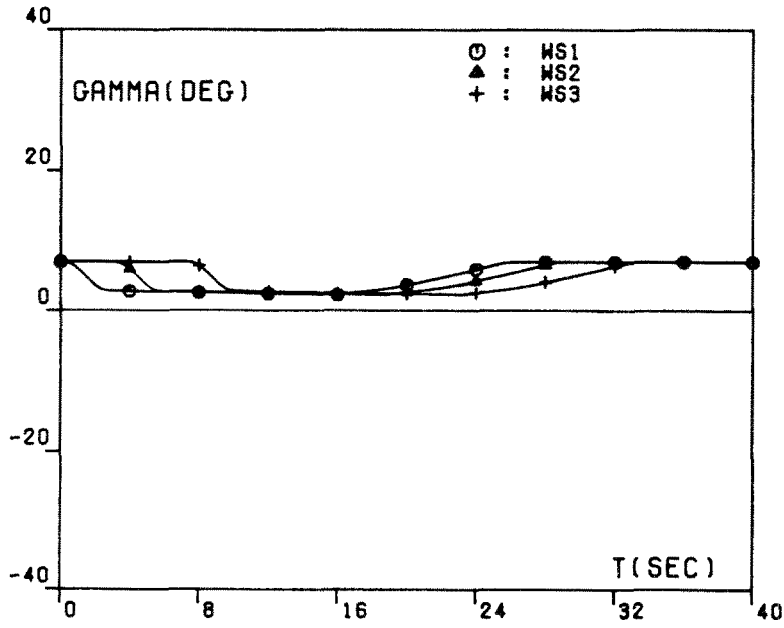

Fig. 7D. Relative path inclination γ versus time t (gamma guidance, effect of the windshear model).

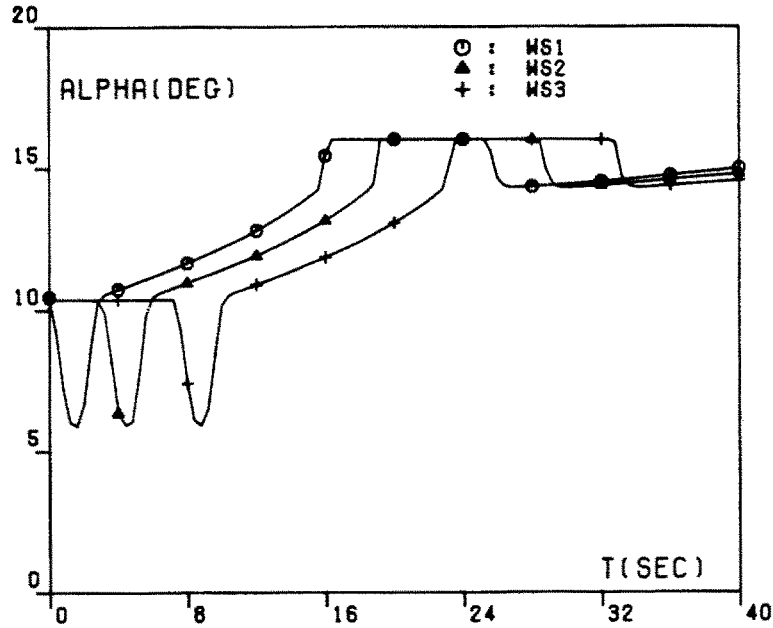

Fig. 7E. Relative angle of attack α versus time t (gamma guidance, effect of the windshear model).

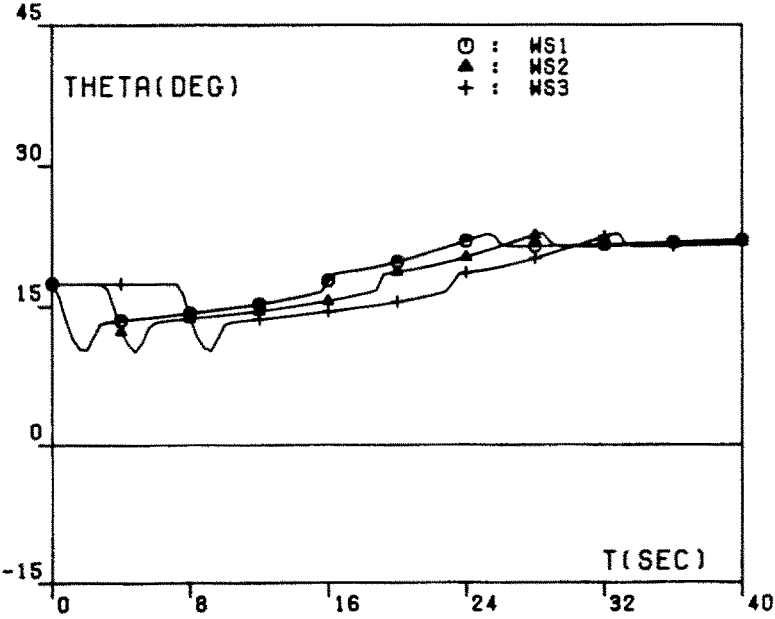

Fig. 7F. Pitch attitude angle θ versus time t (gamma guidance, effect of the windshear model).

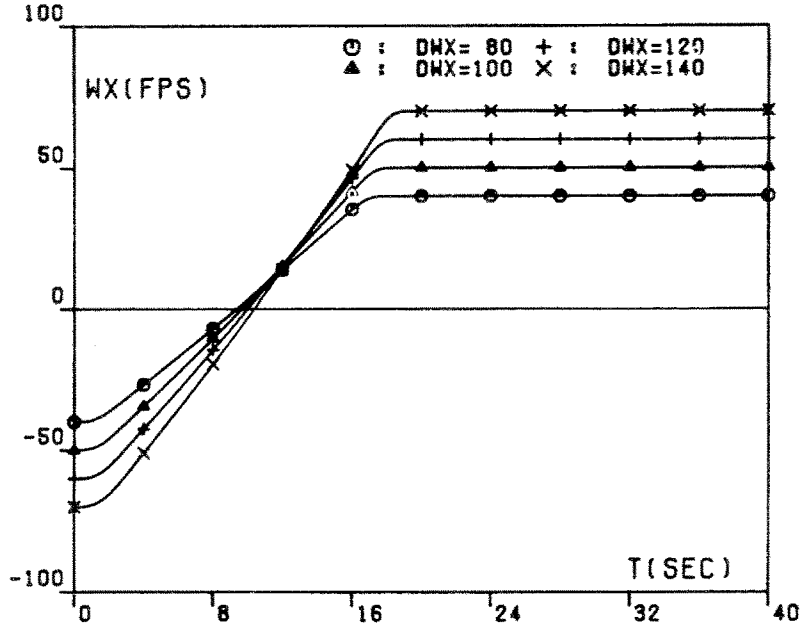

Fig. 8A. Horizontal component of the wind velocity W_x versus time t (gamma guidance, effect of the windshear intensity).

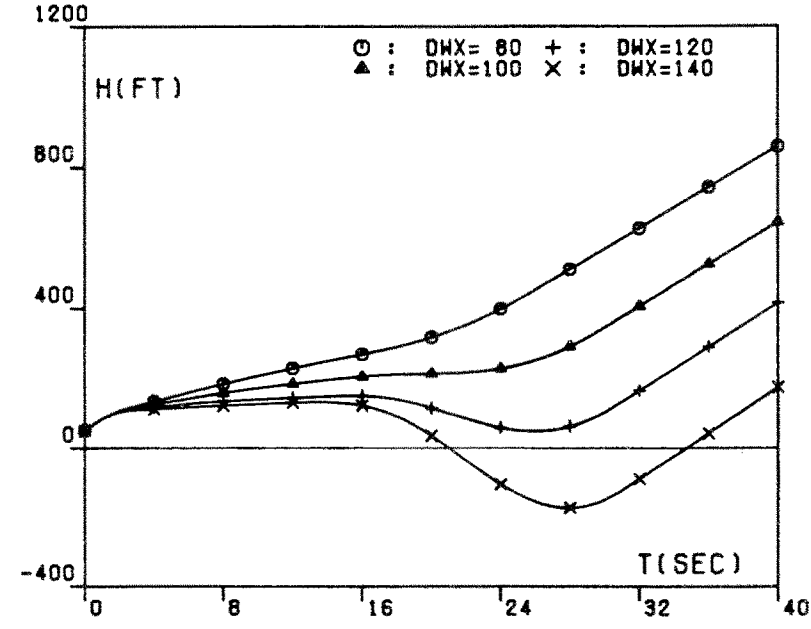

Fig. 8B. Altitude h versus time t (gamma guidance, effect of the windshear intensity).

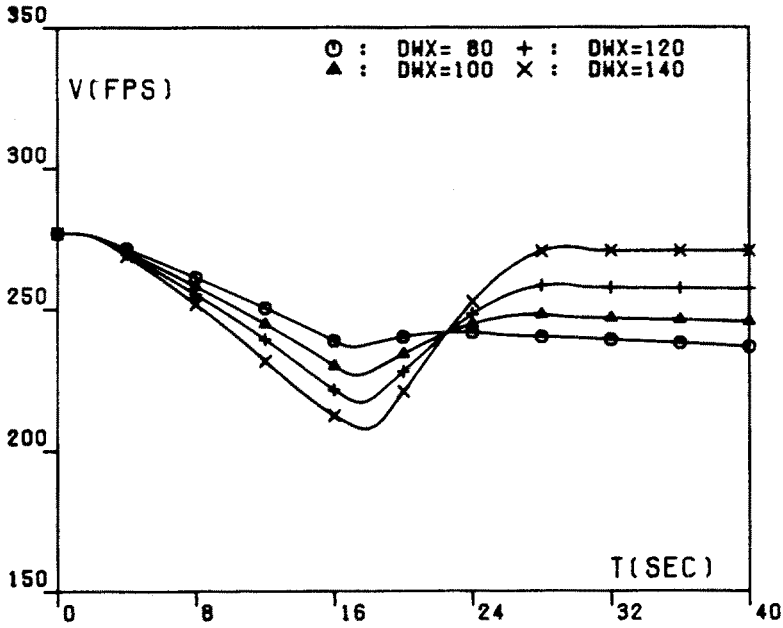

Fig. 8C. Relative velocity V versus time t (gamma guidance, effect of the windshear intensity).

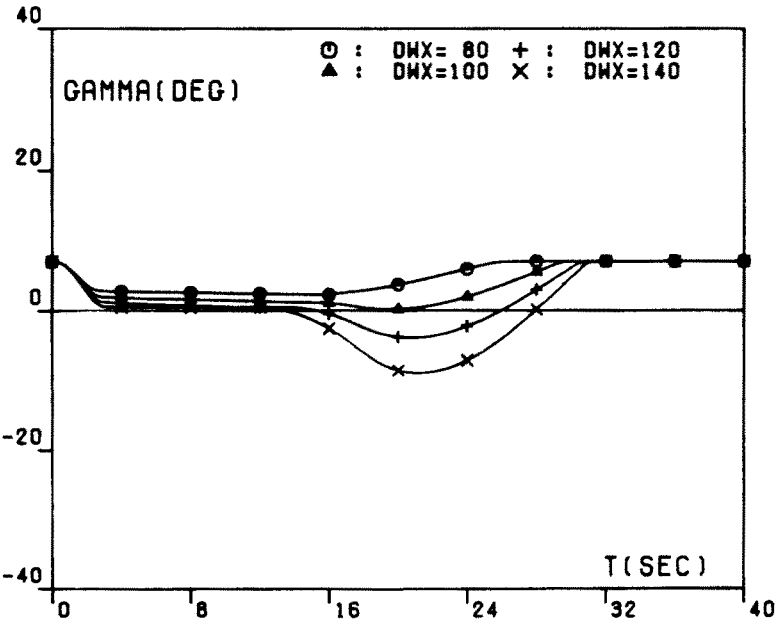

Fig. 8D. Relative path inclination γ versus time t (gamma guidance, effect of the windshear intensity).

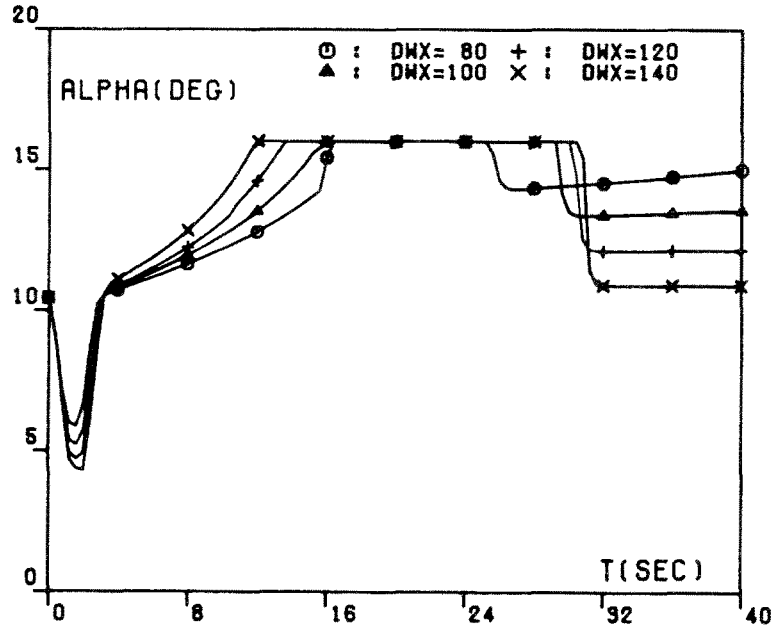

Fig. 8E. Relative angle of attack α versus time t (gamma guidance, effect of the windshear intensity).

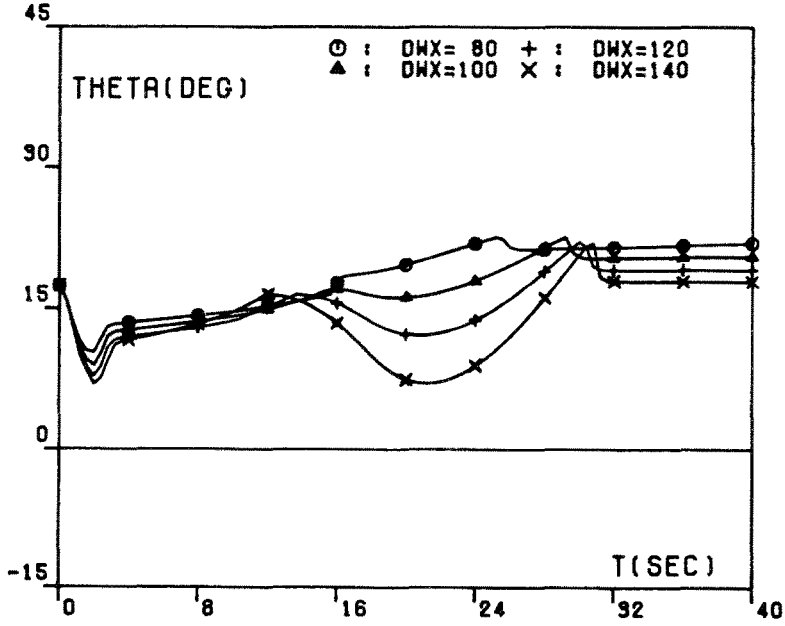

Fig. 8F. Pitch attitude angle θ versus time t (gamma guidance, effect of the windshear intensity).